Keratin 19 expression in hepatocellular carcinoma is regulated by fibroblast-derived HGF via MET-ERK1/2-AP1/SP1 axis

Hyungjin Rhee
Department of Medical Science
The Graduate School, Yonsei University

Keratin 19 expression in hepatocellular carcinoma is regulated by fibroblast-derived HGF via MET-ERK1/2-AP1/SP1 axis

Directed by Professor Young Nyun Park

The Doctoral Dissertation
submitted to the Department of Medical Science,
the Graduate School of Yonsei University
in partial fulfillment of the requirements for the degree of
Doctor of Philosophy

Hyungjin Rhee

December 2016

This certifies that the Doctoral Dissertation of Hyungjin Rhee is approved.

Thesis Supervisor: Young Nyun Park

Thesis Committee Member #1: Myeong-Jin Kim

Thesis Committee Member #2: Jin-Sub Choi

Thesis Committee Member #3: Ho-Geun Yoon

Thesis Committee Member #4: Hyun Goo Woo

The Graduate School

Yonsei University

December 2016

ACKNOWLEDGEMENTS

I would like to show my deep gratitude to Professor Young Nyun Park, who is my thesis director. Her encouragement, guidance and support in every step of the process enabled me to develop an understanding of the subject.

And I especially would like to thank to the members of my thesis committee, Prof. Myeong-Jin Kim, Prof. Jin-Sub Choi, Prof. Ho-Geun Yoon and Prof. Hyun Goo Woo. With their critical comments and thoughtful suggestions, this thesis could be produced with completeness.

I am also very grateful to Prof. Ki Whang Kim, and Prof. Myeong-Jin Kim for the suggestion of Physician-Scientist program. Without their guidance, I would not able to challenge the unaccustomed academic field.

I owe my deep gratitude to Jeong Eun Yoo, Young-Joo Kim, Ji Hae Nahm, Hyun Ho Han, Won Kyu Kim, and Hye-Young Kim, and all colleagues of the Department of Pathology, for healthy criticism, suggestions, and cooperation that gave inspiration to this paper.

In addition, I want to show an appreciation to my lovely wife, my daughter and son, parents, parents-in-law, and all family members who always support me.

TABLE OF CONTENTS

LIST OF FIGURES

LIST OF TABLES

ABSTRACT

Keratin 19 expression in hepatocellular carcinoma is regulated by fibroblast-derived HGF via MET-ERK1/2-AP1/SP1 axis

Hyungjin Rhee

Department of Medical Science
The Graduate School, Yonsei University

(Directed by Professor Young Nyun Park)

Background: Keratin 19 (KRT19) has been shown to be a stem/progenitor marker of liver cells and poor prognostic factor for hepatocellular carcinoma (HCC). We recently reported that HCCs with abundant fibrous stroma (scirrhous HCC) show expression of KRT19. The regulatory mechanism of KRT19 in HCC, however, is not well understood.

Materials and methods: We investigated regulatory mechanisms of KRT19 expression in HCC using an *in vitro* model of paracrine interactions between hepatic stellate cell (hTERT-HSC) and HCC cell lines (HepG2, SNU423). The regulatory axis of KRT19 was validated in tissue microarrays of human HCC tissue (n=339).

Results: The hepatic stellate cell line (hTERT-HSC) upregulated transcriptional and translational levels of KRT19 in both HCC cell lines (HepG2, SNU423) via paracrine interaction. Conditioned media (CM) from hTERT-HSC upregulated KRT19 expression via activation of the MEK-ERK1/2 pathway. Hepatocyte growth factor (HGF) from the hTERT-HSC CM and subsequent activation of c-MET in the HCC cell lines were responsible for ERK1/2 activation and KRT19 upregulation. Luciferase reporter assay revealed that AP1 and SP1 binding sites in KRT19 promoter

are important to transgene expression. AP1 family proteins, JUN and FOSL1, and SP1, which are downstream transcriptional activators of ERK1/2, were found to be activators of KRT19 gene expression. Multikinase inhibitors, including sorafenib and crizotinib, which inhibit MET and ERK1/2 pathways, eliminated the previously observed, CM-induced upregulation of KRT19. In human HCC tissue, the expression of KRT19 was correlated with MET and FOSL1 expression, as well as amounts of tumor fibrous stroma.

Conclusion: The expression of KRT19 in HCC is regulated by fibrous tumor stroma therein via a HGF-MET-ERK1/2-AP1 and SP1 axis. Our results provide insights into the molecular background of aggressive, KRT19-positive HCC.

Key words: Keratin 19, Cancer-associated fibroblast, Hepatocyte growth factor, MET protooncogene, Fos-related antigen 1

Keratin 19 expression in hepatocellular carcinoma is regulated by fibroblast-derived HGF via MET-ERK1/2-AP1/SP1 axis

Hyungjin Rhee

Department of Medical Science
The Graduate School, Yonsei University

(Directed by Professor Young Nyun Park)

I. INTRODUCTION

Keratin 19 (KRT19) is a small, type I cytokeratin (approximately 40kDa); it lacks the tail domain common among cytokeratins.[1] KRT19 is normally expressed in the simple epithelia of various organs, including the breast, trachea, gastrointestinal track, and pancreas.[2,3] It is also expressed in neoplastic tissues, including carcinomas of the breast, lung, stomach, colon, and pancreas.[4] In normal liver tissue, hepatocytes express KRT8 and KRT18, while cholangiocytes and bipotential hepatic progenitor cells additionally express KRT7 and KRT19.[5]

Like normal hepatocytes, most of hepatocellular carcinomas (HCCs) do not express KRT19. Those that do expresses KRT19 (10-28% of HCCs)[6-8] show invasive phenotype[8,9] and they also were related with poor outcomes when treated with hepatic resection,[8,10] or radiofrequency ablation.[11] Interestingly, KRT19 protein expression or KRT19 expression-related signature has emerged as predictors of HCC recurrence and survival after liver transplantation.[12,13] Accordingly, KRT19 expression is

considered a marker of poor prognosis in HCC patients treated with all three currently available, curative treatments of HCC.[14,15]

Despite the clinical significance of KRT19 expression in HCC, the regulatory mechanism of KRT19 expression is not well understood. Previously, a subset of KRT19-positive HCCs were considered to be of hepatic progenitor cell origin, in which KRT19 is normally expressed.[16] However, recent lineage-tracing rodent models of HCC demonstrated that KRT19-positive HCC cells were of mature hepatocyte origin and were not observed in the early clonal expansion of hepatocarcinogenesis.[17,18] These results suggest that KRT19 expression is an acquired phenotype during hepatocarcinogenesis, and thus, it is plausible that KRT19 expression might be regulated by microenvironmental factors. We previously reported that HCCs with abundant fibrous stroma (namely, "scirrhous HCC") commonly express KRT19.[19] In light of these results, we hypothesized that KRT19 expression in HCCs might be regulated by fibrous stromal components therein.

Cancer-associated fibroblasts have been shown to contribute to an aggressive cancer phenotype, facilitating invasiveness, proliferation, and immune suppression.[20] In HCC, cancer-associated fibroblasts are recruited and transdifferentiated from peritumoral myofibroblasts by crosstalk with tumor cells.[21] Hepatic myofibroblasts are a heterogenous group of cells, and activated hepatic stellate cells are one of major source of hepatic myofibroblasts.[22,23]

Here, we established an *in vitro* interaction model of HCC cells and cancer-associated fibroblasts using HCC and hepatic stellate cell lines. We discovered that hepatic stellate cell-derived hepatocyte growth factor (HGF) and subsequent activation of the MET-MEK-ERK1/2 pathway activates KRT19 transcription via AP1 (JUN/FOSL1) and SP1 transcription factors. This regulatory axis was validated in a large HCC cohort (n=339) with immunohistochemical staining. Our results provide better understanding of the molecular background of KRT19-positive HCCs.

II. MATERIALS AND METHODS

1. Cell lines and reagents

HepG2, Hep3B, and PLC/PRF/5 lines were purchased from American Type Culture Collection (ATCC; Manassas, VA, USA), and Huh7, SNU182, SNU423, and SNU475 cell lines were purchased from Korean Cell Line Bank (Seoul, Korea). hTERT-HSC and LX-2 cell lines were obtained as gifts from David Brenner[24] and Scott Friedman[25], respectively. Cell lines were maintained in Dulbecco Modified Eagle Medium supplemented with 10% fetal bovine serum and penicillin/streptomycin (Invitrogen, Carlsbad, CA, USA). U0126 and sorafenib were purchased from Cell Signaling Technology (Danvers, MA, USA); mithramycin A was purchased from Tocris Bioscience (Bristol, UK); and SCH772984, SU11274, PHA-665752, and crizotinib were purchased from Selleckchem (Houston, TX, USA).

2. Generation of conditioned media and enzyme-linked immunosorbent assay (ELISA)

For conditioned media generation, two hepatic stellate cell lines (hTERT-HSC, LX-2) were seeded on 150-mm plates at a confluency of 70-80%, incubated with complete media for 3 days, filtered through a 0.45-μm syringe filter, and stored at -20°C until ready for use. Concentrations of HGF were determined with a human HGF ELISA kit purchased from R&D systems (Minneapolis, MN, USA).

3. Quantitative real time PCR

Total RNA was extracted from cell line samples with a RNeasy Mini kit (Qiagen, Valencia, CA, USA). RNA was quantified with Nanodrop (Thermo Scientific, Pittsburgh, PA, USA), and a total of 1 μg of RNA was subsequently subjected to DNase I treatment and subsequent cDNA synthesis using M-MLV Reverse Transcriptase (Invitrogen). Quantitative real-time PCR reactions were performed on the Step One Plus system using Taqman or SYBR-based detection reagents (Applied Biosystems, Foster City, CA, USA). The primers and probe sets used in the PCR

reactions are listed in Table 1. All quantitative real-time PCR reactions were carried out with the standard curve method, unless otherwise described. Serially diluted HepG2 cDNA was used as standard for quantitation.

Table 1. Primer sequences for PCR reaction

Gene	Forward primer	Reverse primer	Probe
Primer/probe sets for probe-based detection			
ACTB	GTCCCCCAACTTGAGATGTATG	AAGTCAGTGTACAGGTAAGCC	CTGCCTCCACCCACTCCCA
KRT19	AGCCACTACTACACGACCAT	TTGGTTCGGAAGTCATCTGC	TGCCACCATTGAGAACTCCAGGATT
Primer sets for SYBR-based detection			
ACTB	CACCATTGGCAATGAGCGGTTC	AGGTCTTTGCGGATGTCCACGT	
JUN	CCTTGAAAGCTCAGAACTCGGAG	TGCTGCGTTAGCATGAGTTGGC	
JUNB	CGATCTGCACAAGATGAACCACG	CTGCTGAGGTTGGTGTAAACGG	
FOS	GCCTCTCTTACTACCACTCACC	AGATGGCAGTGACCGTGGGAAT	
FOSB	TCTGTCTTCGGTGGACTCCTTC	GTTGCACAAGCCACTGGAGGTC	
JUND	ATCGACATGGACACGCAGGAGC	CTCCGTGTTCTGACTCTTGAGG	
FOSL1	GGAGGAAGGAACTGACCGACTT	CTCTAGGCGCTCCTTCTGCTTC	
FOSL2	AAGAGGAGGAGAAGCGTCGCAT	GCTCAGCAATCTCCTTCTGCAG	

(continued)

Gene	Forward primer	Reverse primer	Probe
Primer sets for SYBR-based detection			
SP1	ACGCTTCACACGTTCGGATGAG	TGACAGGTGGTCACTCCTCATG	
Primer sets for chromatic immunoprecipitation assay			
AP1 (-2021 from TSS)	TCAGGCCAGAAAAACAGAGC	AGAGCCCAAGAGGGAGAAAG	
SP1 (-72 from TSS)	GCCCATATTTGCTCTCAGGA	GAGCAACCCTGGTCTCAGAA	

4. Western blot analysis and phospho-receptor tyrosine kinase array

Cell line samples were washed with phosphate-based saline two times and then lysed with cell extraction buffer (Invitrogen). Protein concentrations were determined with a BCA Protein Assay kit (Thermo Scientific). Next, 30 μg of lysate were loaded to precast Bis-Tris gel, after which electrophoresis and dry blotting to a PVDF membrane were performed according to the manufacturer's instructions (Invitrogen). The membrane was blocked for 30 mins in room temperature (tris-based saline, 0.1% tween 20, 5% bovine serum albumin), and then incubated with primary antibody for 4°C overnight. Protein expression was detected with horseradish peroxidase-conjugated secondary antibodies (Cell Signaling Technology), chemiluminescent substrate (Thermo Scientific), and X-ray film (AGFA). The antibodies used in the western blot analysis are listed in Table 2. The phospho-receptor tyrosine kinase array was purchased from R&D systems and performed in accordance with the manufacturer's protocol.

Table 2. List of antibodies

Antibody	Source	Application
β-actin (mouse mAb, C-4)	Santa Cruz Biotechnology (Santa Cruz, CA, USA)	Western blot
phospho-Akt (Ser473, rabbit mAb, clone D9E)	Cell signaling (Danvers, MA, USA)	Western blot
Akt (rabbit mAb, clone C67E7)	Cell signaling (Danvers, MA, USA)	Western blot
phospho-ERK1/2 (Thr202/Tyr204, rabbit mAb, clone D13.14.4E)	Cell signaling (Danvers, MA, USA)	Western blot
ERK1/2 (rabbit mAb, clone 137F5)	Cell signaling (Danvers, MA, USA)	Western blot
FAP (rat mAb, clone D8)	Vitatex (Stony Brook, NY, USA)	Western blot
phospho-FOSL1 (Ser265, rabbit mAb, clone D22B1)	Cell signaling (Danvers, MA, USA)	Western blot
FOSL1 (rabbit mAb, clone D80B4)	Cell signaling (Danvers, MA, USA)	Western blot
FOSL1 (mouse mAb, C-12)	Santa Cruz Biotechnology (Santa Cruz, CA, USA)	Chromatin immunoprecipitation, Immunohistochemistry
HGF (goat pAb)	R&D system (Minneapolis, MN, USA)	Neutralization, Immunofluorescence
HGF (rabbit pAb)	Sigma-Aldrich (St. Louis, MO, USA)	Immunohistochemistry
phospho-JNK (Thr183/Tyr185, rabbit mAb, clone 81E11)	Cell signaling (Danvers, MA, USA)	Western blot
JNK (rabbit pAb)	Cell signaling (Danvers, MA, USA)	Western blot

(continued)

Antibody	Source	Application
phospho-JUN (Ser73, rabbit mAb, clone D47G9)	Cell signaling (Danvers, MA, USA)	Western blot, Chromatin immunoprecipitation
JUN (rabbit mAb, clone 60A8)	Cell signaling (Danvers, MA, USA)	Western blot
KRT19 (mouse mAb, clone RCK108)	Abcam (Cambridge, MA, USA) or Dako (Glostrup, Denmark)	Western blot, Immunohistochemistry
Lamin B (rabbit pAb)	Abcam (Cambridge, MA, USA)	Western blot
phospho-MET (Tyr1234/1235, rabbit mAb, clone D26)	Cell signaling (Danvers, MA, USA)	Western blot
MET (rabbit mAb, clone D1C2)	Cell signaling (Danvers, MA, USA)	Western blot, Immunofluorescence
MET (rabbit mAb, clone SP44)	Ventana Medical Systems, Inc., Tucson, AZ, USA	Immunohistochemistry
Myc-Tag (mouse mAb, clone 9B11)	Cell signaling (Danvers, MA, USA)	Western blot
phospho-p38 (Thr180/Tyr182, rabbit mAb, clone D3F9)	Cell signaling (Danvers, MA, USA)	Western blot
p38 (rabbit mAb, clone D13E1)	Cell signaling (Danvers, MA, USA)	Western blot
α-SMA (mouse mAb, clone 1A4)	Dako (Glostrup, Denmark)	Western blot, Immunohistochemistry
SP1 (rabbit mAb, clone D4C3)	Cell signaling (Danvers, MA, USA)	Western blot, Chromatin immunoprecipitation
phospho-STAT3 (Tyr705, rabbit mAb, clone D3A7)	Cell signaling (Danvers, MA, USA)	Western blot
STAT3 (mouse mAb, clone 124H6)	Cell signaling (Danvers, MA, USA)	Western blot
Vimentin (mouse mAb, clone Vim 3B4)	Dako (Glostrup, Denmark)	Western blot

5. Plasmids, siRNA, and transfection

pLenti-puro, pLenti-MetGFP, Tet-pLKO-puro, psPAX2, and pMD2.G were purchased from Addgene (Cambridge, MA, USA). pLenti-puro was obtained as a gift from Ie-Ming Shih (Addgene plasmid # 39481),[26] pLenti-MetGFP a gift from David Rimm (Addgene plasmid # 37560). Tet-pLKO-puro a gift from Dmitri Wiederschain (Addgene plasmid # 21915),[27] and psPAX2 and pMD2.G gifts from Didier Trono (Addgene plasmid # 12259, # 12260). Empty expression vectors, pCMV-myc and p3xFLAG-CMV-10 were purchased from Clontech (Palo Alto, CA, USA) and Sigma-Aldrich (St. Louis, MO, USA), respectively. We cloned the coding DNA sequence (CDS) of the MET gene from pLenti-MetGFP, and inserted to pLenti-puro vector (pLenti-puro-MET). The CDSs of MEK1 and ERK1 were amplified from complementary DNA (cDNA) from HepG2 and cloned into pCMV-myc (pCMV-myc-MEK1, pCMV-myc-ERK1). To obtain a constitutively active form of MEK1, we substituted two serine residues (S218, S222) to aspartate using site-specific mutagenesis (pCMV-myc-MEK1 S218D/S222D). The CDSs of JUN, FOSL1, and SP1 were cloned from HepG2 cDNA into p3xFLAG-CMV-10 vector. The heterodimeric fusion protein of JUN and FOSL1 (JUN~FOSL1)[28] were generated by inserting glycine rich linker between the CDSs of JUN and FOSL1 and then also cloned into p3xFLAG-CMV-10 vector. All siRNA or shRNA target sequences were taken from the RNAi consortium collection (Sigma-Aldrich); they are listed in Table 3. Transient transfection of plasmid or siRNA was performed with Lipofectamine 3000 reagent according to the manufacturer's instructions.

To establish inducible HGF-knockdown hTERT-HSC, we inserted synthesized oligo harboring shRNA sequences to Tet-pLKO-puro vector. Lentiviruses were produced in HEK293FT cells (Invitrogen) with Tet-pLKO-puro, psPAX, and pMD2.G plasmids and Lipofectamine 3000 reagent. The virus transduced hTERT-HSC cell lines were selected with puromycin (1 μg/mL). For HGF knockdown, 1 μg/mL of doxycycline was treated for 48 hrs.

Table 3. shRNA/siRNA target sequences for gene knockdown

Name	Type	Target sequence	etc
shHGF-1	shRNA	GTGATACCACACCTACAATAG	Cloned to Tet-pLKO-puro vector
shHGF-2	shRNA	TTTGTCCGAGTAGCATATTAT	Cloned to Tet-pLKO-puro vector
siJUN-1	siRNA	AGATGGAAACGACCTTCTA	
siJUN-2	siRNA	GTCATGAACCACGTTAACA	
siJUND-1	siRNA	AGCATGCTGAAGAAAGACGC	
siJUND-2	siRNA	GAAAGTCCTCAGCCACGTCAA	
siFOS-1	siRNA	GCGGAGACAGACCAACTAGAA	
siFOS-2	siRNA	ACCTATCTGGGTCCTTCTATG	
siFOSL1-1	siRNA	GTACGTCGAAGGCCTTGTGAA	
siFOSL1-2	siRNA	CTGTACCTTGTATCTCCCTTT	
siFOSL2-1	siRNA	GCAGTGAGTATTGGAAGACTT	
siFOSL2-2	siRNA	CACGGCCCAGTGTGCAAGATT	

6. Dual luciferase assay

Two reporter plasmids, pGL4.10 and pNL1.1.TK, and a dual luciferase assay kit were purchased from Promega (Madison, WI, USA). The 5' flanking region of KRT19 gene, -2885 from +41, relative to the transcription start site (corresponds to -2946 from -20 relative to first ATG), was amplified from HepG2 genomic DNA and cloned into pGL4.10 vector. Using PCR, the KRT19 promoter insert was serially deleted at the interval of 100-400 base pairs, from the 5' end. To investigate functionally relevant transcription factor binding sites, the putative transcription factor binding sites were mutated using site-specific mutagenesis. All promoter constructs were sequenced to verify the sequence. HepG2 and SNU423 cells were seeded to 96-well white plates at a density of 10,000 cells per well. A total of 50 ng of reporter plasmids were transfected with Lipofectamine 3000 reagent at the following ratio of pGL4 vector: pNL vector = 500 : 1. At 48 hrs post transfection, dual luciferase assays were performed according to the manufacturer's protocol.

7. Oligo pull-down and chromatic immunoprecipitation assay

For oligo pull-down assay, 26 base-pair-long, double-stranded KRT19 promoter fragments containing the AP1 binding site (5'-ATAAGGGAA*TGACTCA*GAGCTGACCA-3' biotin) or a mutant AP1 binding site (5'-ATAAGGGAA*AAACCCG*GAGCTGACCA-3' biotin) were synthesized. KRT19 promoter fragments containing the SP1 binding site (5'–CTCAGATAT*CCGCCCC*TGACACCATT–3' biotin) or a mutant SP1 binding site (5'– CTCAGATAT*CCGTTCC*TGACACCATT– 3' biotin) was also synthesized. Next, 100 pico-mole of double-stranded DNA fragment was incubated with 250 μg streptavidin-conjugated magnetic bead (Invitrogen) and 500 μL of binding/wash buffer (5 mM Tris-HCl [pH 7.4], 0.5 mM EDTA, 1M NaCl) in a rotator. A total of 1 mg of nuclear lysate from HepG2 or SNU423 was pre-cleared with 125 μg of streptavidin-conjugated magnetic beads (Invitrogen) and 2.5 μg of Poly(dI-dC) (Sigma-Aldrich). The promoter fragment-magnetic bead complex was washed and then incubated with pre-cleared nuclear lysate for 2 hrs in a cold room. The magnetic

beads were washed five times with binding/wash buffer, and the DNA-binding proteins were eluted by boiling in 2X LDS sample buffer (Invitrogen) and analyzed by western blot.

Chromatic immunoprecipitation assay was carried out with a SimpleChIP Plus enzymatic chromatic IP kit (Cell signaling) following the manufacturer's instruction. The primer sets used in the PCR reaction are listed in Table 1.

8. Immunofluorescence staining

For immunofluorescence staining, cells on cell culture slide (SPL Life Sciences, Pocheon, Republic of Korea) were fixed with 4% formaldehyde, washed with PBS, and permeabilized and blocked with blocking buffer (PBS, 1% BSA, and 0.3% Triton X-100). They were then incubated with primary antibody with blocking buffer at 4°C overnight. After washing, the slides were incubated with fluorochrome-conjugated secondary antibodies (Invitrogen) for 1 hr at room temperature. The slides were then washed and mounted with antifade mounting medium with DAPI counterstain (Vector Laboratories, Burlingame, CA, USA).

9. Human hepatocellular carcinoma samples, and clinicopathologic and immunohistochemical analyses

We enrolled total 339 HCC patients who did not undergo any kind of preoperative treatment before hepatic resection. Consecutive HCC samples were obtained by hepatic resection between March 2006 and February 2011 at Severance Hospital, Yonsei University Medical Center. The clinicopathological characteristics of the cohort are described in Table 4. The representative paraffin-embedded sections of HCC were used for tissue microarray construction and immunohistochemical analysis. For TMA construction, two core biopsies of 2 mm in diameter were taken from individual HCC donor paraffin blocks and arranged into recipient TMA blocks using a trephine apparatus (Superbiochips Laboratories, Seoul, Korea).

Immunohistochemical staining for KRT19, HGF, MET, and FOSL1 was performed using an automated staining system (Ventana Medical Systems, Inc.,

Tucson, AZ, USA). α-smooth muscle actin (αSMA) was stained using an Envision kit (Dako) according to the manufacturer's instructions. All slides were counter-stained with hematoxylin. Detailed information on criteria for immunohistochemical analysis is described in Table 5.

The clinical outcomes of the patients were retrospectively obtained by reviewing the electronic medical record system at Severance Hospital. The last update of the patient cohort was September 2016. The endpoints were defined as follows. Disease-specific survival was defined as time from surgery to death in patients with HCC involving >50% of the liver, HCC with extensive portal vein tumor thrombosis, or HCC with extrahepatic metastasis.[29] Disease-free survival was defined as the time from surgery to initial diagnosis of recurrence regardless of location. This study was approved by the Institutional Review Board of Severance Hospital, and the requirement for informed consent was waived.

Table 4. Clinicopathologic characteristics of hepatocellular carcinoma cohort (n=339)

Clinicopathologic features	Value
Age (year)	56 (48-63)
Gender (male/female)	277 (82%) / 62 (18%)
Etiology (hepatitis B/hepatitis C/alcohol/unknown)	277 (82%) / 18 (5%) / 15 (4%) / 29 (9%)
Cirrhosis	187 (55%)
Serum aspartate transaminase (IU/L)	30 (24-41)
Serum alanine transaminase (IU/L)	31 (22-45)
Serum albumin (g/dL)	4.4 (4.1-4.7)
Serum platelet (1000/μL)	163.0 (131.0-208.0)
Serum alpha-fetoprotein (IU/mL) [1]	22.8 (4.3-221.3)
Serum PIVKA-II (AU/mL)[2]	80.0 (32.0-491.8)
Tumor pathology	
Diameter of largest tumor (cm)	3.0 (2.2-4.5)
Differentiation (Edmonson-Steiner grade I/II/III)	26 (8%) / 246 (73%) / 67 (20%)
Capsule formation (absent/partial/complete)	59 (17%) / 182 (54%) / 98 (29%)
Microvascular invasion	194 (57%)
Tumor multiplicity	44 (13%)
TNM stage (I/II/III)	122 (36%) / 200 (59%) / 17 (5%)
Preoperative treatment (none / preoperative locoregional therapy)	339 (100%) / 0 (0%)

Table 5. Criteria for immunohistochemistry analysis

Antibody	Score	Definition
KRT19	Negative / Positive	Positive: cytoplasmic expression, moderate or strong intensity, ≥5% of tumor cells
HGF, MET	Negative / Positive	Positive: membranous expression, moderate or strong intensity, ≥5% of tumor cells
FOSL1	Negative / Positive	Positive: nuclear expression, moderate or strong intensity, ≥5% of tumor cells
αSMA-positive cancer associated fibroblast	Proportion (%)	Stromal fibroblast proportion in tumor tissue, moderate or strong intensity

10. Statistical analysis

Statistical analyses were performed using SPSS software (version 23.0, SPSS Inc., Chicago, IL, USA). Mann-Whitney U test, chi-square test, or Fisher's exact test were used as deemed appropriate. Survival analyses were performed by the Kaplan-Meier method and log rank test.

III. RESULTS

1. KRT19 expression is upregulated by paracrine factors from hepatic stellate cells

Correlation between fibrous stromal components and KRT19 expression was confirmed in our TMA cohort (n=339). Expression of KRT19 protein increased along with increases in α-smooth muscle actin (αSMA)-positive cancer-associated fibroblasts (Figure 1A and B).

To establish an *in vitro* model of interactions between cancer-associated fibroblasts and epithelial tumor cells in HCC, we tested two hepatic stellate cell lines; hTERT-HSC and LX-2. hTERT-HSC showed more fibroblast-like morphology, and higher expression of fibroblast activation-related markers including FAP and αSMA,[30] compared to LX-2 (Figure 2A and B). Interestingly, conditioned media (CM) from hTERT-HSC induced increased expression of KRT19 in HepG2, whereas CM from LX-2 did not (Figure 2C).

Next, we treated HepG2 and SNU423 cell lines with CM from hTERT-HSC for 12-72 hrs. The CM from hTERT-HSC increased mRNA and protein expression of KRT19, and the difference was apparent at 24-72 hrs (Figure 3A). We also conducted indirect co-culture using permeable cell culture inserts of 1-μm pore size. Sharing of the culture media between the HCC cell lines and hTERT-HSC increased expression of KRT19 mRNA and protein in HepG2 and SNU423 (Figure 3B). Both CM treatment and indirect co-culture resulted in similar features of cell scattering and elongation (Figure 3C). These results suggest that paracrine factors from hTERT-HSC regulate the expression of KRT19 in HCC cell lines.

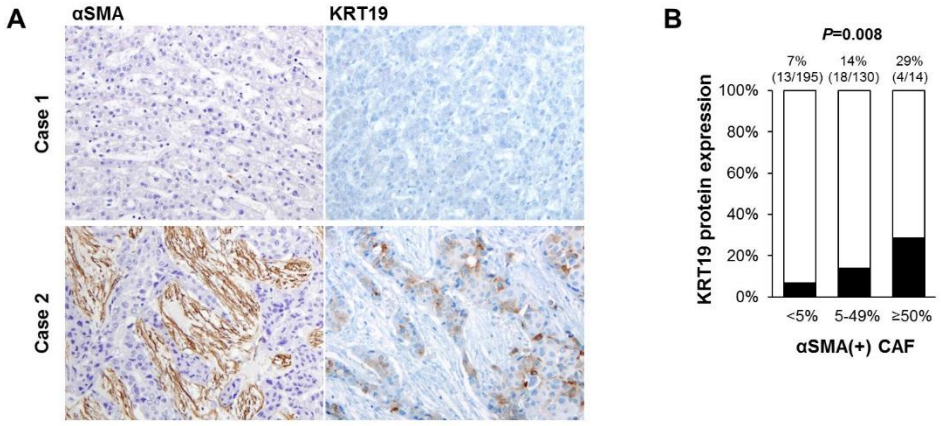

Figure 1. Correlation between cancer-associated fibroblast and KRT19 expression in hepatocellular carcinoma (HCC) tissues. A) Representative cases of HCC with or without α-smooth muscle actin (αSMA)-positive cancer-associated fibroblasts. B) Correlation between αSMA-positive cancer-associated fibroblast and KRT19 protein expression.

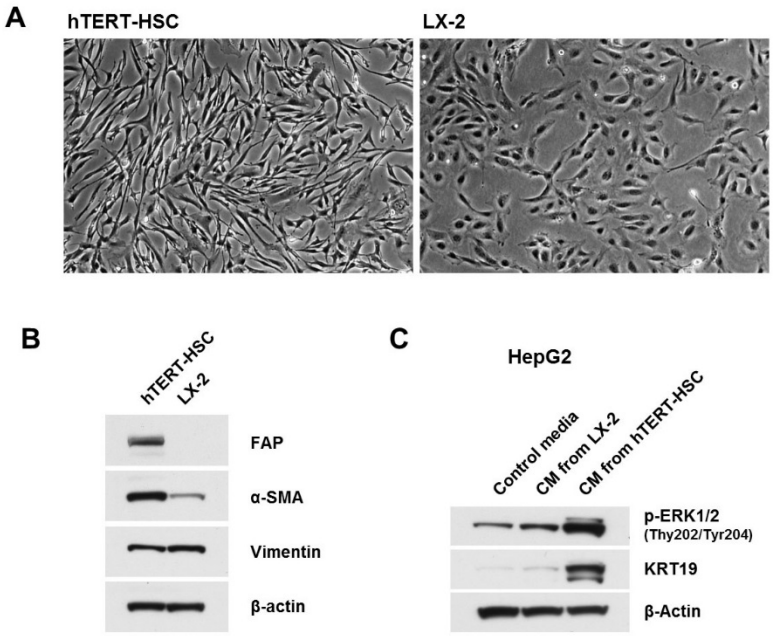

Figure 2. Characteristics of hepatic stellate cell lines. A) Cell morphology of two hepatic stellate cell lines, hTERT-HSC and LX-2. B) Western blot analysis of fibroblast activation-related markers in hTERT-HSC and LX-2. C) Protein expression change of phospho-ERK1/2 and KRT19 of HepG2, following treatment with conditioned media (CM) from hTERT-HSC or LX-2.

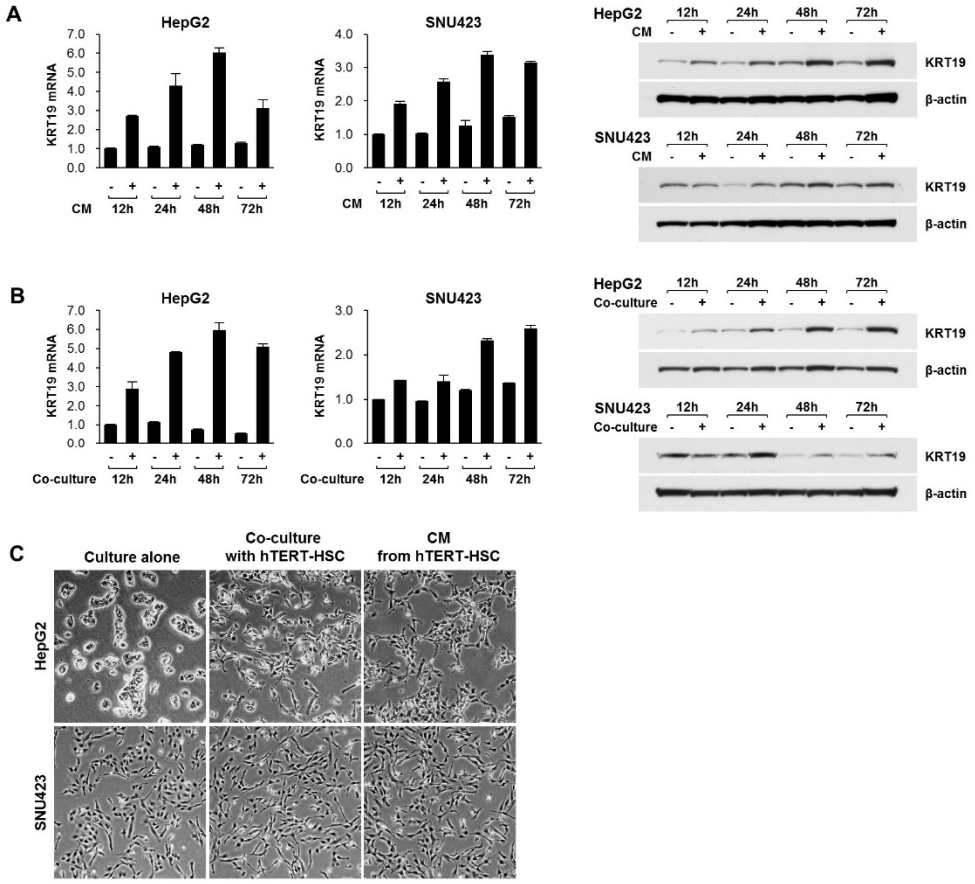

Figure 3. KRT19 expression in HCC is upregulated by paracrine factors from hepatic stellate cells. A) mRNA and protein expression level of KRT19 after hTERT-HSC conditioned media (CM) treatment. The HCC cells (HepG2 and SNU423) were harvested at the indicated times, and mRNA and protein expression was analyzed by qRT-PCR or western blot. Bar graph represents mean ± SD. B) mRNA and protein expression levels of KRT19 after co-culture with hTERT-HSC. C) Morphologic changes in HepG2 and SNU423 induced by co-culture with hTERT-HSC or CM from hTERT-HSC.

2. Conditioned media regulates KRT19 expression through MEK-ERK1/2 pathway

KRT19-positive HCC is associated with invasive phenotype and poor prognosis. Accordingly, we hypothesized that KRT19 expression would be regulated by an oncogenic signaling pathway. To investigate the signaling pathways intervening in the upregulation of KRT19 upon treatment with CM from hTERT-HSC, we screened the activation statuses of representative oncogenic signaling pathways, including MAPK, AKT, and STAT3. The CM treatment induced the phosphorylation of ERK1/2 in both HepG2 and SNU423 cells and STAT3 in HepG2 only. Other signaling pathways, including p38 MAPK, JNK, and AKT, were unchanged (Figure 4A). STAT3 inhibitor (S3I-201) treatment decreased KRT19 expression in HepG2 cells, but not in SNU423 cells, suggesting that the STAT3 pathway is not a common regulator of KRT19 for both cell lines (Figure 4B).

When the MEK-ERK1/2 pathway was inhibited by MEK inhibitor (U0126) or ERK1/2 inhibitor (SCH772984),[31] the observed CM-treatment-induced KRT19 upregulation vanished in HepG2 and SNU423 cells (Figure 5A). KRT19 expression also increased with 12-O-Tetradecanoylphorbol-13-acetate (TPA) treatment, and combination of MEK or ERK1/2 inhibitor with TPA decreased KRT19 expression (Figure 5B). To further confirm the regulation of KRT19 expression by MEK-ERK1/2 pathway, constitutively active form of MEK1 (S218D/S222D) and ERK1 wild type were overexpressed in two HCC cell lines.[32] To obtain more apparent results, we used HepG2 and SNU475 cells in an overexpression experiment, instead of SNU423, because the transfection efficiency of SNU423 is quite low, compared to other cells (Figure 5C). The overexpression of MEK1 S218D/S222D and ERK1 increased KRT19 expression by two- to six-fold (Figure 5D). Taken together, CM increased KRT19 expression in HCC cell lines through MEK-ERK1/2 pathway.

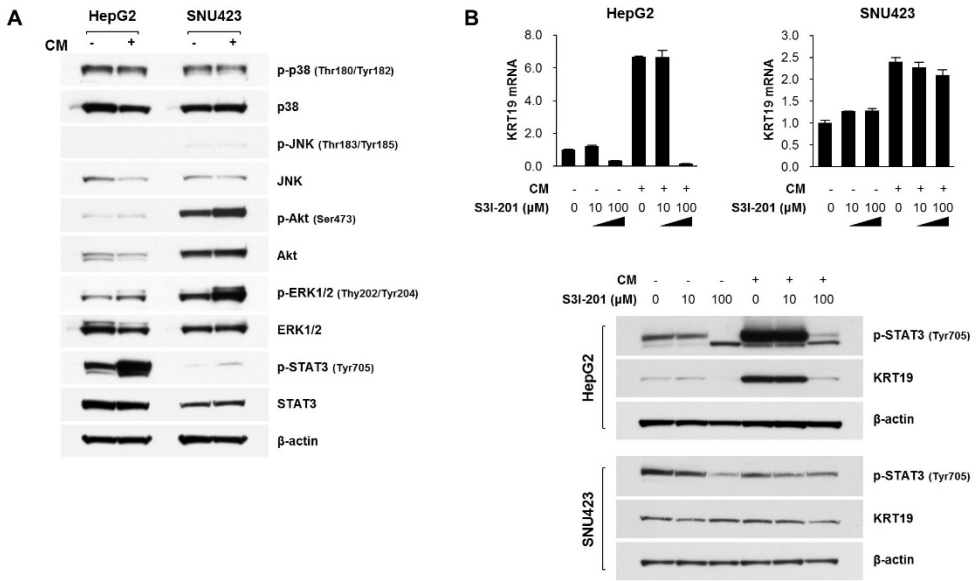

Figure 4. Screening of activation status of selected oncogenic pathways after conditioned media (CM) treatment. A) The activation status of selected oncogenic pathways in HepG2 and SNU423 cells by CM from hTERT-HSC. B) mRNA and protein levels of KRT19 after 24 hrs CM treatment combined with/without the STAT3 inhibitor SI3-201 in HepG2 and SNU423 cells. mRNA and protein expression was analyzed by qRT-PCR or western blot. Bar graph represents mean ± SD.

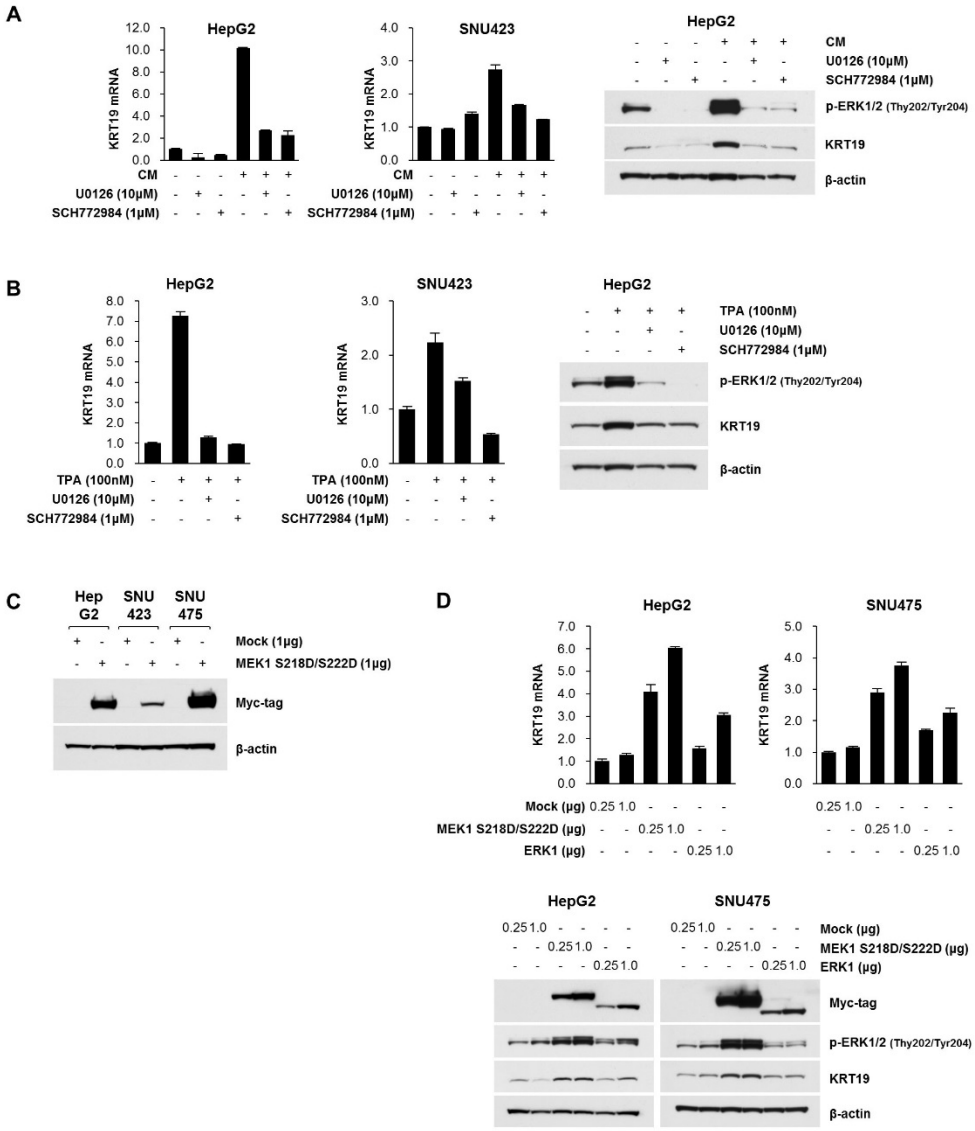

Figure 5. Conditioned media (CM) regulates KRT19 expression through the MEK-ERK1/2 pathway. A) mRNA and protein level of KRT19 after CM treatment combined with/without MEK or ERK inhibitor. mRNA and protein expression was analyzed by qRT-PCR or western blot. Bar graph represents mean ± SD. B) mRNA and protein levels of KRT19 after 24 hrs of treatment with 12-O-Tetradecanoylphorbol-13-acetate (TPA) combined with MEK1 or ERK1/2 inhibitor. C) Transient protein expression by plasmid transfection, MEK1 (S218D/S222D), in

HepG2, SNU423, and SNU475 cells. The amounts of plasmid used in transfection (per 35mm dish) are indicated. D) mRNA and protein upregulation of KRT19 in HepG2 and SNU475, by transient expression of constitutively active MEK1 (S218D/S222D) or ERK1.

3. Hepatocyte growth factor (HGF) in hTERT-HSC conditioned media (CM) upregulates KRT19 via MET and MEK-ERK1/2 pathway

To specify which paracrine factor and receptor activates the MEK-ERK1/2 pathway in HCC cells, we performed phospho-receptor tyrosine kinase array for HepG2 and SNU423 cell lines. The results of the array reflected increased phosphorylation of three common receptors: MET, ALK, and FGFR3 (Figure 6A). We decided to further investigate MET and its well-known ligand, hepatocyte growth factor (HGF), since several reports have shown that HGF is secreted by cancer-associated fibroblasts in HCC.[30,33] We confirmed the activation of phosphorylated MET upon treatment with CM in HepG2 and SNU423 cells using western blot (Figure 6B). HGF concentrations, determined by ELISA, were much higher in CM of hTERT-HSC (>10ng/mL), compared to CM from HepG2 and SNU423 (<0.2ng/mL) (Figure 6C). Treatment with recombinant HGF induced KRT19 upregulation in both HCC cell lines, and combined treatment with MAPK inhibitors decreased HGF-induced KRT19 upregulation (Figure 6D).

Additionally, HGF concentrations in CM from another hepatic stellate cell line, LX-2, were very low (<0.1ng/mL). The CM from hTERT-HSC (high HGF concentration) increased KRT19 expression, whereas CM from LX-2 (low HGF concentration) did not (Figure 7A). In addition, HCC cell lines with low MET expression, including SNU182 and PLC/PRF/5, showed low KRT19 expression (Figure 7B). The transient overexpression of MET in SNU475 increased phospho-MET and phospho-ERK1/2, as well as KRT19 at the mRNA and protein levels. In PLC/PRF/5, overexpression of MET also increased phospho-MET and phospho-ERK1/2 and mRNA levels of KRT19. Protein levels of KRT19 were undetectable (Figure 7C).

To determine whether HGF is indeed responsible for CM-induced KRT19 upregulation, we established a doxycycline-inducible knockdown version of hTERT-HSC (hT-shHGF-1, hT-shHGF-2). Two days of doxycycline treatment (1μg/mL) prior to CM generation efficiently knockdowned HGF concentration (7.2 ng/mL *vs.* 0.17 ng/mL in hT-shHGF-1, 8.4 ng/mL *vs.* 0.13 ng/mL in hT-shHGF-2, Figure 8A).

Treatment of HepG2 and SNU423 cells with CM from hT-shHGF-1 or hT-shHGF-2 without doxycycline upregulated KRT19 expression at both transcriptional and translational levels in the cells; treatment with CM from hT-shHGF-1 or hT-shHGF-2 with doxycycline, however, did not (Figure 8B). Also, doxycycline reversed the CM-induced cell scatter in hT-shHGF-1 and 2 (Figure 8C). Further, HGF-neutralization with anti-HGF immunoglobulin also reversed the CM-induced KRT19 upregulation and cell scatter (Figure 8D and E). When MET selective inhibitors (SU11274 and PHA-665752) were combined with CM, the upregulation of KRT19 also diminished (Figure 8F). Our result suggests that HGF paracrine signaling from hepatic stellate cells upregulates KRT19 via MET and the MEK-ERK1/2 pathway.

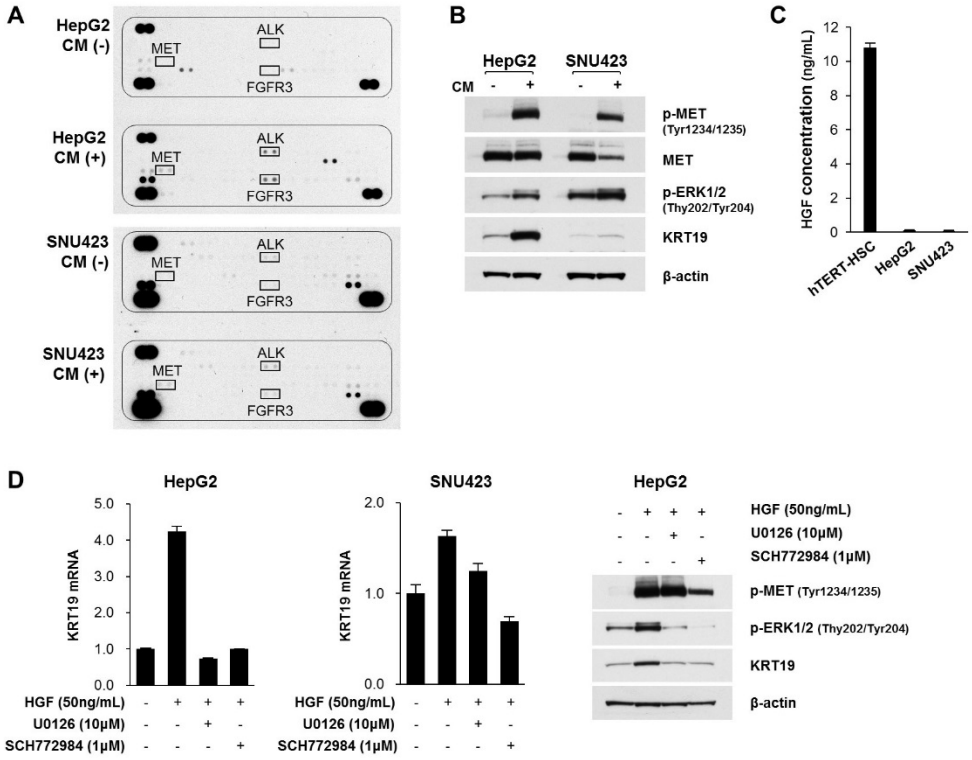

Figure 6. Hepatocyte growth factor (HGF) upregulates KRT19 via MET and MEK-ERK1/2 pathway. A) The phosphorylation status of receptor tyrosine kinases of HepG2 and SNU423 with conditioned media (CM) from hTERT-HSC. The increased phosphorylation of three receptors (MET, ALK, and FGFR3) were commonly observed in HepG2 and SNU423 cells. B) Increased phosphorylation of MET following CM treatment was confirmed in HepG2 and SNU423 cells. C) HGF concentrations in CM from hTERT-HSC, HepG2, and SNU423 cells determined by enzyme-linked immunosorbent assay. D) mRNA and protein levels of KRT19 after HGF treatment combined with/without MEK or ERK inhibitor. mRNA and protein expression was analyzed by qRT-PCR or western blot. Bar graph represents mean ± SD.

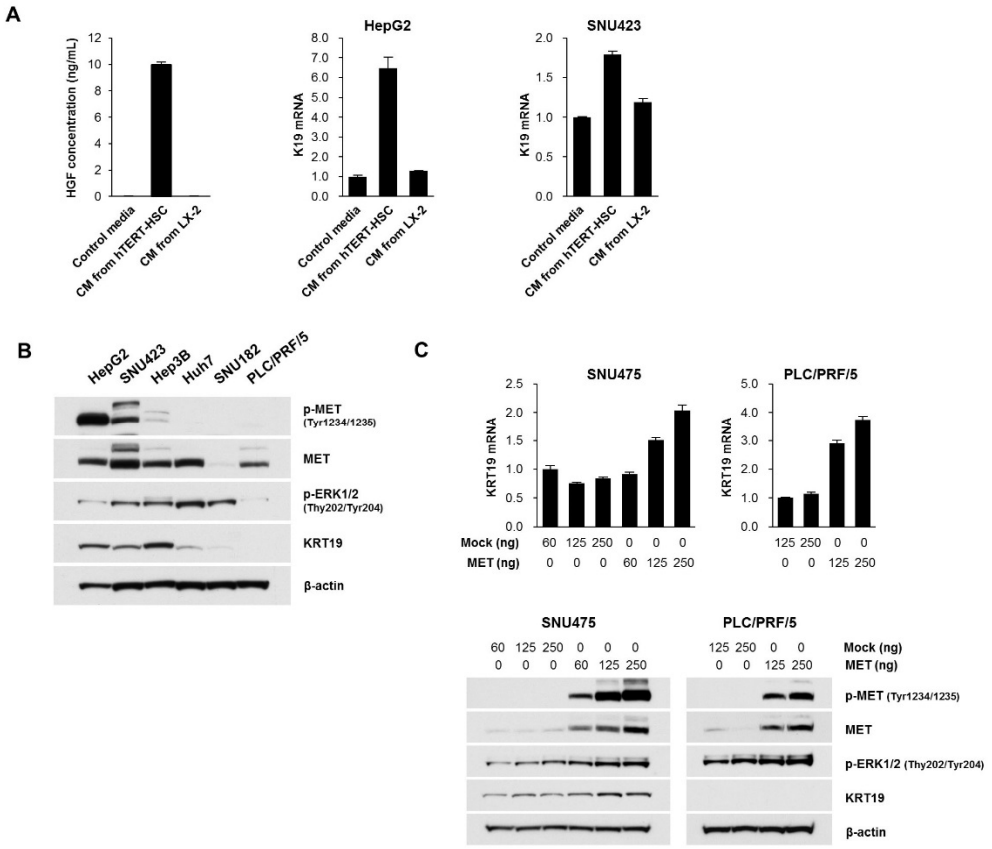

Figure 7. Hepatocyte growth factor (HGF) and MET expression in hepatic stellate cell lines and hepatocellular carcinoma (HCC) cell lines. A) HGF concentrations in complete media (DMEM+10% FBS) and conditioned media (CM) from hTERT-HSC and LX-2. KRT19 mRNA expression of HepG2 and SNU423, after 24 hrs of treatment with CM from hTERT-HSC and LX-2 cells. mRNA expression was analyzed by qRT-PCR. Bar graph represents mean ± SD. B) Western blot analysis of HCC cell lines, showing expression of phospho-MET, MET, phsopho-ERK1/2, and KRT19. C) mRNA and protein expression of KRT19 in SNU475 and PLC/PRF/5 cells, following transient expression of MET. The amounts of plasmids used in transfection (per 35mm dish) were indicated.

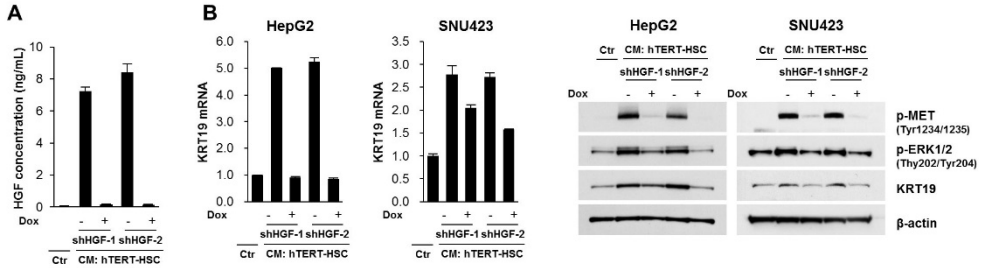

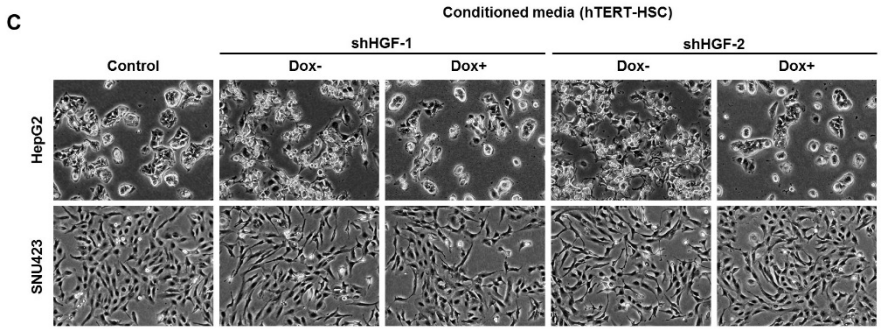

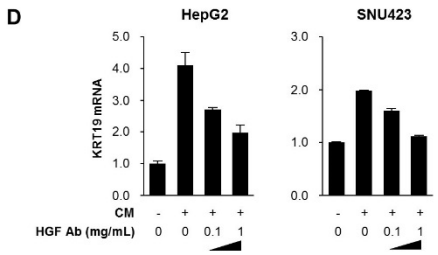

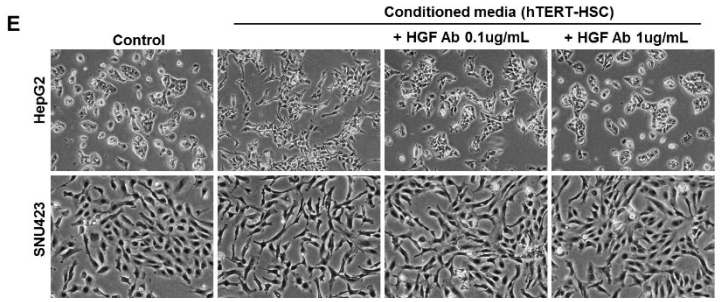

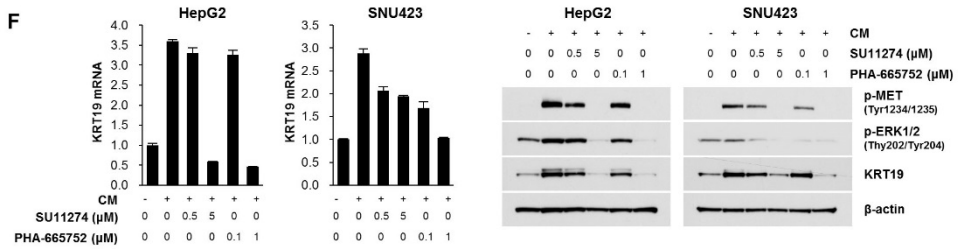

Figure 8. Inhibition of hepatocyte growth factor (HGF) – MET pathway downregulated KRT19 expression. A) HGF concentrations in complete media (DMEM+10% FBS), and conditioned media (CM) from hT-shHGF-1, hT-shHGF-2 stable cell lines with/without doxycycline treatment. B) mRNA and protein levels of KRT19 after treatment with CM from hT-shHGF-1, hT-shHGF-2 stable cell lines with/without doxycycline treatment. mRNA and protein expressions was analyzed by qRT-PCR or western blot. Bar graph represents mean ± SD. C) Morphologic change of HepG2 and SNU423 induced by CM from inducible HGF knockdown stable cell lines established from hTERT-HSC; shHGF-1 and shHGF-2. D) mRNA expression of KRT19 in HepG2 and SNU423, following CM treatment combined with hepatocyte growth factor (HGF) neutralizing antibody. E) Morphologic change of HepG2 and SNU423 induced by CM from hTERT-HSC, combined with HGF neutralizing antibody. F) mRNA and protein levels of KRT19 after CM treatment combined with/without MET inhibitors.

4. AP1 and SP1 transcription factor binding sites in KRT19 promoter are important to KRT19 expression

To determine important *cis*-regulatory elements in KRT19 promoter, we constructed luciferase reporter plasmids of approximately 3kb-long (-2885bp from +41bp relative to transcription start site) and its serial deletion mutants (Figure 9A). We measured the promoter activity of the constructs in HepG2 and SNU423 cells, which showed similar trends in promoter activity between the two. The promoter activity significantly decreased at two segments: between -2167 and -1968 and between -152 and -69. To confirm that those two promoter segments are truly important in KRT19 regulation, we also measured the promoter activity of segmental deletion constructs of Δ2167-1968 and Δ152-69. The constructs elicited a >70% decrease in promoter activity for Δ2167-1968 and >25% for Δ152-69 (Figure 9B). The putative transcription factor binding sites at -2167~-1968 and -152~-69 were searched in online programs (PROMO; http://alggen.lsi.upc.es, and Tfsitescan; http://www.ifti.org/cgi-bin/ifti/Tfsitescan.pl), the mutant constructs of AP1, MAZ, ELK, ETS, and SP1 binding sites were generated by site-specific mutagenesis (Figure 4C). Of these mutant constructs, mutants of the -2021 AP1 site and -72 SP1 site demonstrated significantly reduced activity. Therefore, AP1 and SP1, which are known as downstream transcriptional activators of ERK1/2, were identified to be important in KRT19 regulation.

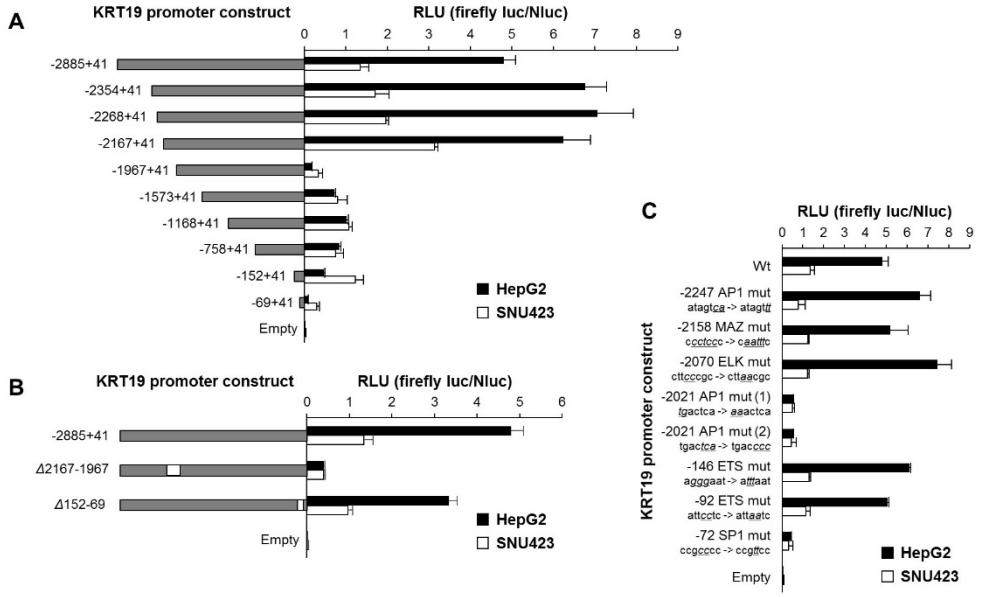

Figure 9. AP1 and SP1 transcription factor binding sites in KRT19 promoter are important to KRT19 expression. A) Luciferase reporter assay result of KRT19 promoter constructs. Approximately 3kb-long KRT19 promoter and its serial deletion constructs were tested in HepG2 and SNU423 cells, and the firefly luciferase results were normalized with thymidine kinase-promoter driven nano-Luc luciferase results. Bar graph represents mean ± SD. B) Luciferase reporter assay results of KRT19 promoter constructs, in which -2167~-1967 or -152~-69 segments were deleted from full length KRT19 promoter using site-directed mutagenesis. C) Luciferase activity of mutant reporter plasmids, in which putative transcription factor binding sites were altered by site directed mutagenesis from full length KRT19 promoter.

5. JUN, FOSL1, and SP1 are important regulators of KRT19 expression

The AP1 binding site sequence of -2021 in the KRT19 promoter (TGACTCA) is well known as a TPA-responsive element (TRE), to which various heterodimers of JUN and FOS family proteins could bind.[34] To identify specific AP1 proteins that regulate KRT19 in HCC cell lines, we performed siRNA screening for AP1 family members. At first, we screened the transcription levels of seven JUN and FOS genes, including JUN, JUNB, JUND, FOS, FOSB, FOSL1, and FOSL2. Among these seven genes, we selected JUN, JUND, FOSL1, and FOSL2, which showed relatively higher mRNA expression than the other JUN and FOS family genes (Figure 10A). Targeting these genes, transient knock-down with pooled two siRNAs was carried out, and the knock-down efficiency was greater than 80% in all genes (Figure 10B). JUN or FOSL1 knockdown commonly decreased KRT19 expression in HepG2 and SNU423 cells (Figure 10C). To confirm that these results were not off-target effects of the siRNAs, we transfected siRNAs separately. By transfection of siJUN-1, siJUN-2, siFOSL1-1, and siFOSL1-2, JUN and FOSL1 were successfully knockdowned at the transcriptional and translational levels, and declines in KRT19 mRNA followed in both HepG2 and SNU423 cells (Figure 10D and E).

With SP1 inhibitor (mithramycin A) treatment, KRT19 expression was decreased at the transcriptional and translational levels (Figure 11A). Conversely, overexpression of JUN, FOSL1, a heterodimeric fusion protein of JUN and FOSL1 (JUN~FOSL1),[28] and SP1 increased transcription level of KRT19 (Figure 11B). Reportedly, FOSL1 phosphorylation by ERK1/2 comprises proteasomal degradation and increases stability.[35] In accordance with this previous reports, HepG2 and SNU423 cells treated with CM demonstrated increased phosphorylation and protein quantities of FOSL1 (Figure 11C).

To confirm the binding of JUN, FOSL1 and SP1 in KRT19 promoter, we performed DNA pull-down assay and chromatic immunoprecipitation (ChiP). We synthesized 26-bp-long biotinylated double-stranded DNA, mimicking the AP1 and SP1 sites of the KRT19 promoter that we noted (e.g., -2021 AP1 site, and -72 SP1 site). Mutant biotinylated DNAs were also synthesized, in which AP1 or SP1 binding

motifs were altered. Western blot analyses of the DNA binding assay revealed the binding of JUN and FOSL1 to the -2021 AP1 site and SP1 binding to the -72 SP1 site in HepG2 and SNU423 cells (Figure 11D). ChiP assay confirmed the binding of JUN and FOSL1 at the -2021 AP1 site and SP1 at the -72 SP1 site (Figure 11E).

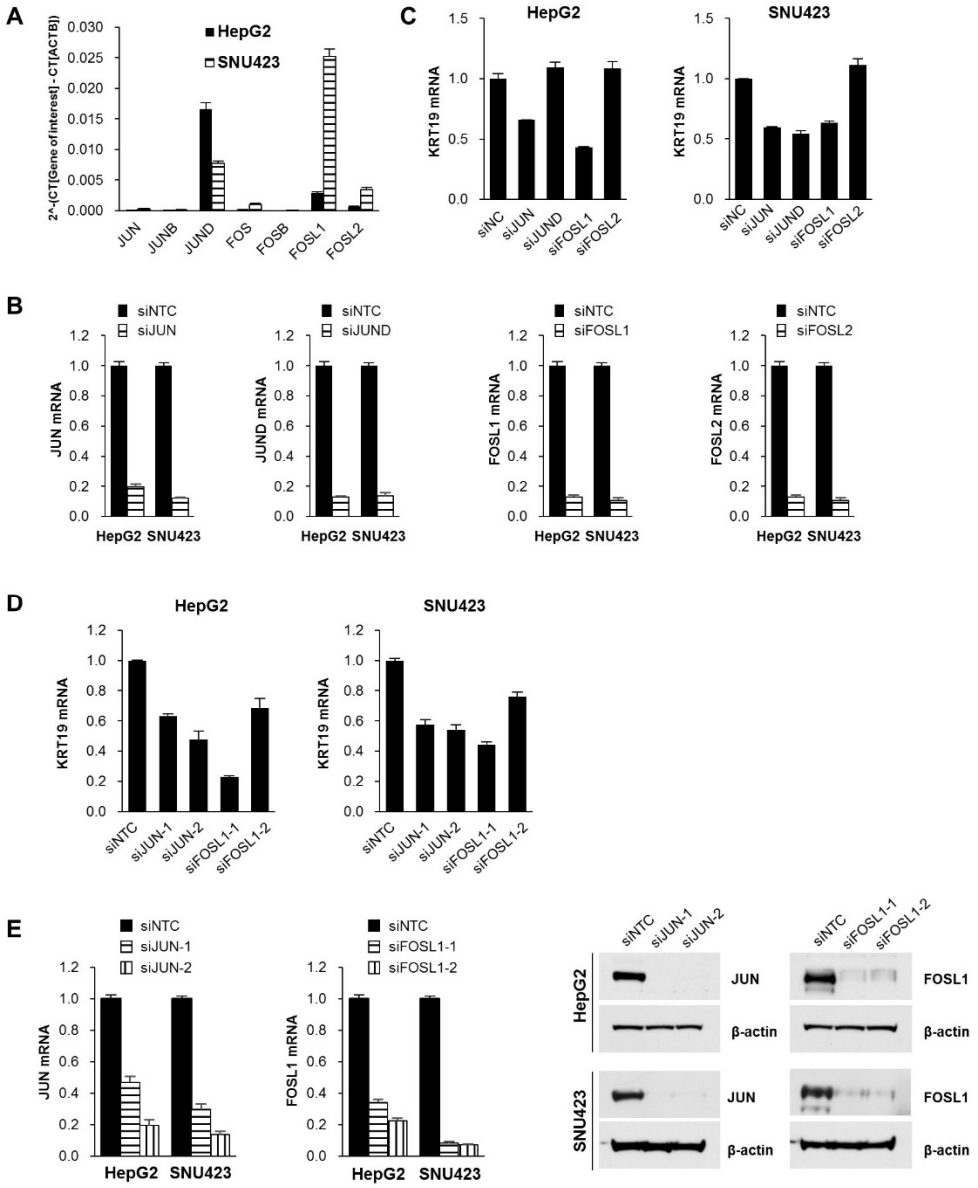

Figure 10. siRNA screening of AP1 family genes demonstrated JUN and FOSL1 is important regulators of KRT19 expression. A) Relative mRNA expression of AP1 family genes that could bind to TPA-responsive elements (TRE). mRNA expression was analyzed by qRT-PCR. Bar graph represents mean ± SD. B) KRT19 mRNA expression after transfection of pooled two siRNAs targeting JUN, JUND, FOSL1, or FOSL2. C) The gene knock-down efficiencies of pooled two siRNAs

targeting JUN, JUND, FOSL1, or FOSL2. D) KRT19 mRNA expression after transfection of siRNAs targeting JUN or FOSL1. E) The gene knock-down efficiencies of siRNAs targeting JUN or FOSL1. The efficiencies were determined by mRNA expression using qRT-PCR and western blot.

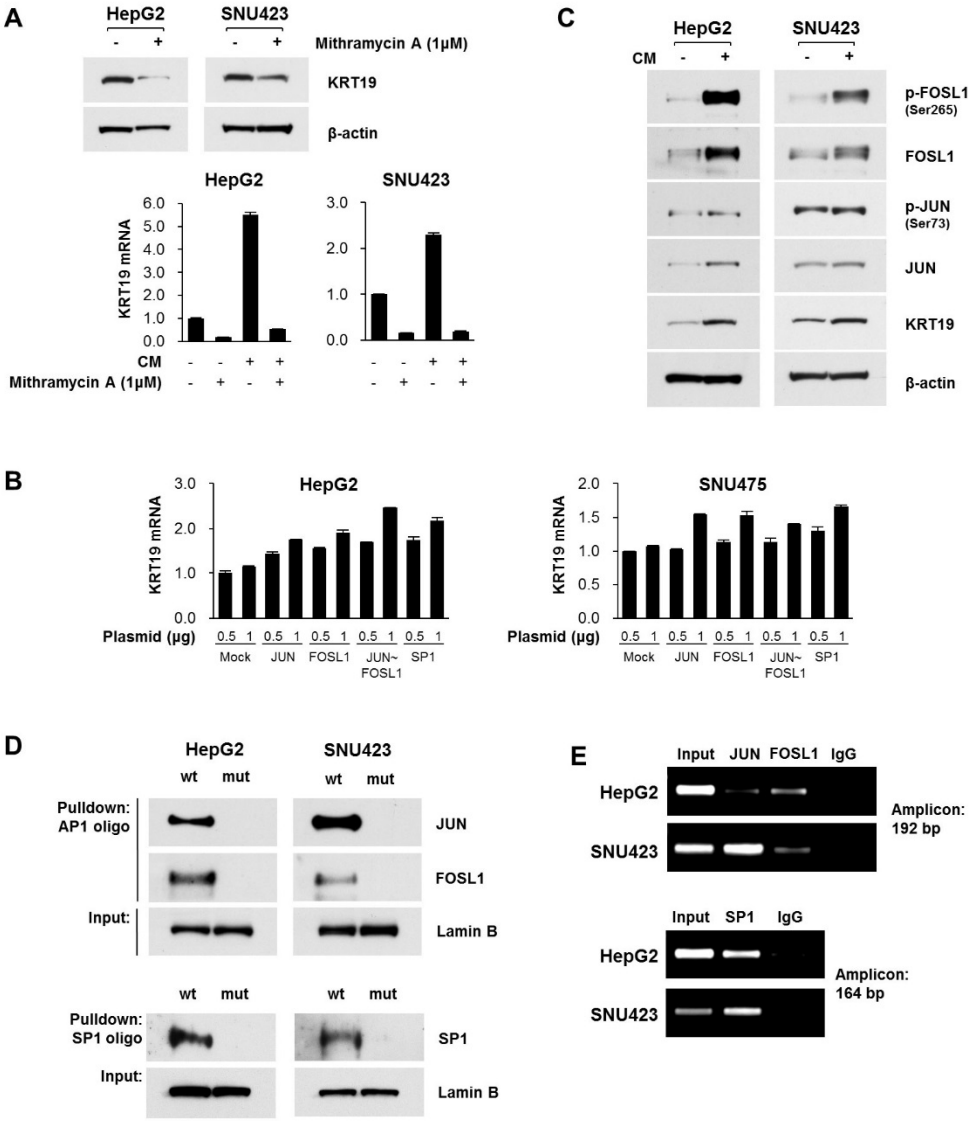

Figure 11. JUN, FOSL1, and SP1 are positive regulators of KRT19 expression. A) mRNA and protein level of KRT19 after 24 hrs of mithramycin A treatment combined with conditioned media (CM). mRNA and protein expression was analyzed by qRT-PCR or western blot. B) mRNA level of KRT19 after transient expression of JUN, FOSL1, JUN~FOSL1 (heterodimeric fusion protein consists of JUN, glycine-rich tether, and FOSL1), and SP1. C) Changes in phosphorylation and quantity of JUN and FOSL1 following 24 hrs of CM treatment in HepG2 and SNU423 cells. D)

Western blot analysis of eluted DNA binding proteins from DNA pulldown assay. Nuclear extracts of HepG2 and SNU423 were incubated with DNA fragments mimicking -2021 AP1 or -72 SP1 binding sites of KRT19. E) Chromatin immunoprecipitation analysis of HepG2 and SNU423 demonstrate JUN and FOSL1 binding at the -2021 AP1 site and SP1 binding at the -72 SP1 site.

6. Crizotinib and sorafenib reduce the expression of KRT19

Two FDA-approved multikinase inhibitors, including crizotinib and sorafenib, were treated to HepG2 and SNU423 cells in combination with CM. Crizotinib can inhibit MET, as well as ALK and ROS1, and sorafenib can suppress MAPK pathway activation by inhibiting RAF.[36,37] When crizotinib was treated without CM, transcription levels of KRT19 were not changed; however, when crizotinib was treated in combination with CM, transcription levels of KRT19 decreased, compared to CM treatment alone. The protein levels of KRT19 showed similar patterns (Figure 12A). Sorafenib treatment reduced the transcriptional and translational levels of KRT19 at the concentration of 10 μm with/without CM combination (Figure 12B).

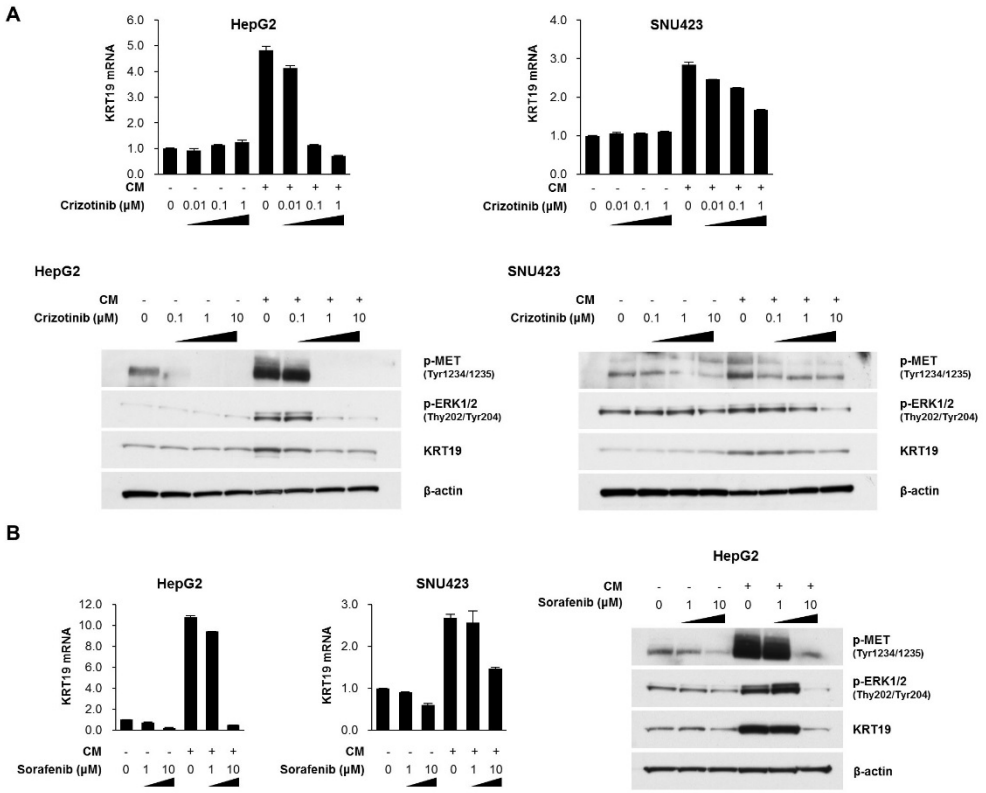

Figure 12. Crizotinib and sorafenib reduce the expression of KRT19. A) mRNA and protein level of KRT19 after treatment with conditioned media (CM) combined with/without crizotinib. mRNA and protein expression were analyzed by qRT-PCR or western blot. Bar graph represents mean ± SD. B) mRNA and protein levels of KRT19 after treatment with CM combined with/without sorafenib.

7. HGF and/or MET expression is correlated with higher expression of KRT19 and FOSL1 in human HCC samples

We assessed expression level of HGF, MET, and their downstream markers, including FOSL1 and KRT19, in our HCC cohort. We also immunostained for phospho-MET in HCC tissues, although none was detected (Figure 13). To assess the stability of phospho-MET in our *in vitro* model, CM-treated HepG2 was harvested at various time points (0 to 30 mins) after media change (CM removed and changed to control media). Western blot analysis revealed a rapid decline in phospho-MET level, whereas MET, FOSL1 and KRT19 expression did not (Figure 14).

Interestingly, HGF expression was more predominant in tumor cells than in cancer-associated fibroblasts (Figure 15A). We also assessed the distribution of HGF in our *in vitro* model. We carried out immunofluorescent staining of HGF in cell lines. HGF is weakly stained in hTERT-HSC cells, but strongly stained in CM-treated HCC cell lines (Figure 15B). In HepG2 cells treated with CM, HGF was observed in intracellular space, serially increased in amounts, and co-localized with MET, suggesting that intracellular HGF in HepG2 came from CM and exists as a complex with MET (Figure 15C). In HCC tissue, HGF was observed in a cytoplasm predominant pattern or membrane predominant pattern. The membrane predominant pattern of HGF was well-correlated with KRT19 expression, whereas the cytoplasmic pattern of HGF was not (Figure 16).

Therefore, membranous distributions of HGF and MET, nuclear expression of FOSL1, and cytoplasmic expression of KRT19 were scored (Figure 17A). The membranous distribution of HGF was well correlated with the presence of cancer-associated fibroblasts (≥5%) (P=0.008), while the membranous MET expression was not (P=0.635) (Figure 17B). KRT19 expression was associated with HGF and FOSL1 (Figure 17C, $P<0.001$, and P=0.001, respectively). When HCC cases were categorized according to HGF and MET status, FOSL1 and KRT19 expression was most frequently observed in the HGF and MET double positive group and least frequently observed in the HGF and MET double negative group (Figure 17D, $P<0.001$ at both). HGF or MET positive patients showed favorable disease-specific

survival and disease-free survival, compared to HGF and MET double negative patients (Figure 17E, P=0.015 and P=0.011, respectively).

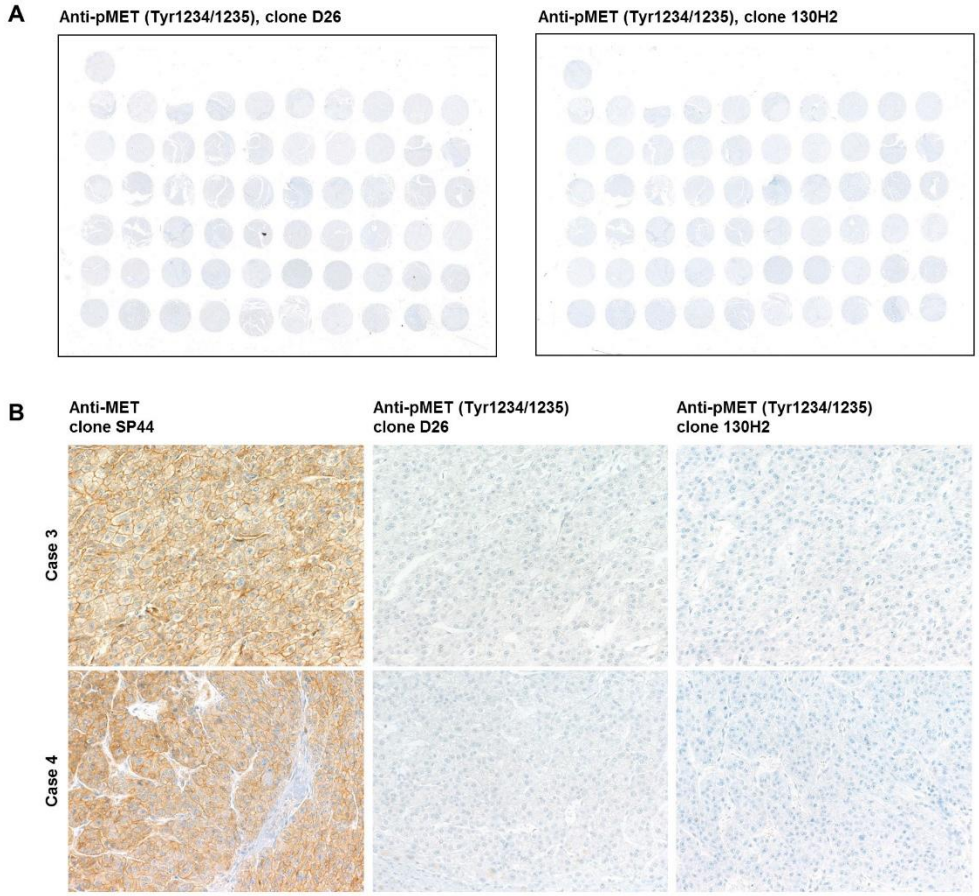

Figure 13. Immunohistochemical staining results for phospho-MET. (A) Immunohistochemical staining results for two different rabbit monoclonal phospho-MET antibodies in a representative tissue microarray slide. (B) Two representative cases with strong MET expression exhibited negative immunohistochemical staining result for phospho-MET.

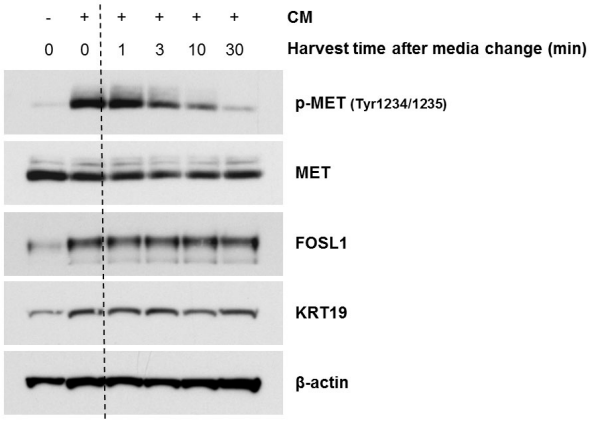

Figure 14. Rapid decline in phospho-MET levels after removal of conditioned media (CM). Western blot analysis of expressions of phospho-MET, MET, FOSL1, and KRT19 in HepG2 cells harvested at various time points (0 to 30 min).

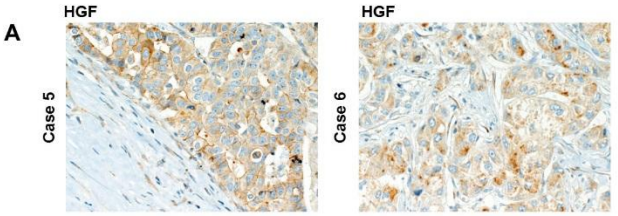

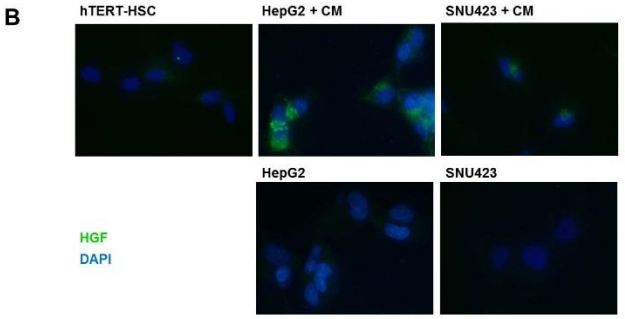

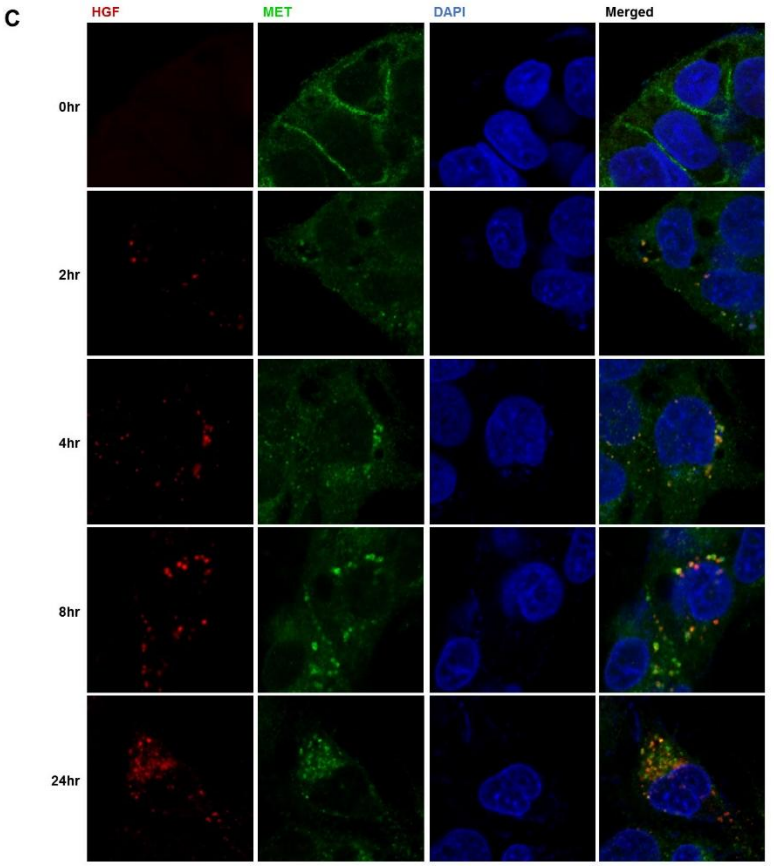

Figure 15. Distribution of hepatocyte growth factor (HGF) in hepatocellular carcinoma (HCC) tissues and the *in vitro* model. A) Representative HCC tissue samples with positive expression of HGF. B) Distribution of HGF in hepatic stellate cell lines and HCC cell lines, including HepG2 and SNU423. C) Distribution of HGF and MET in HepG2 cells, in various time points after conditioned media (CM) treatment.

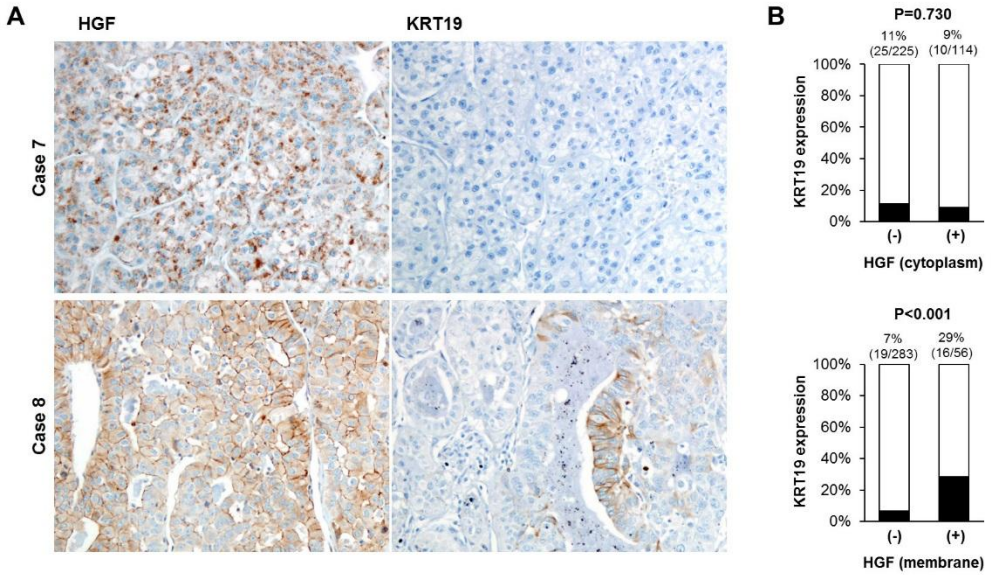

Figure 16. Two distinct patterns of subcellular localization of hepatocyte growth factor (HGF) in hepatocellular carcinoma (HCC) tissues. A) Representative HCC tissue samples with cytoplasmic or membranous distribution of HGF. B) The association between the subcellular localization pattern of HGF and KRT19 expression.

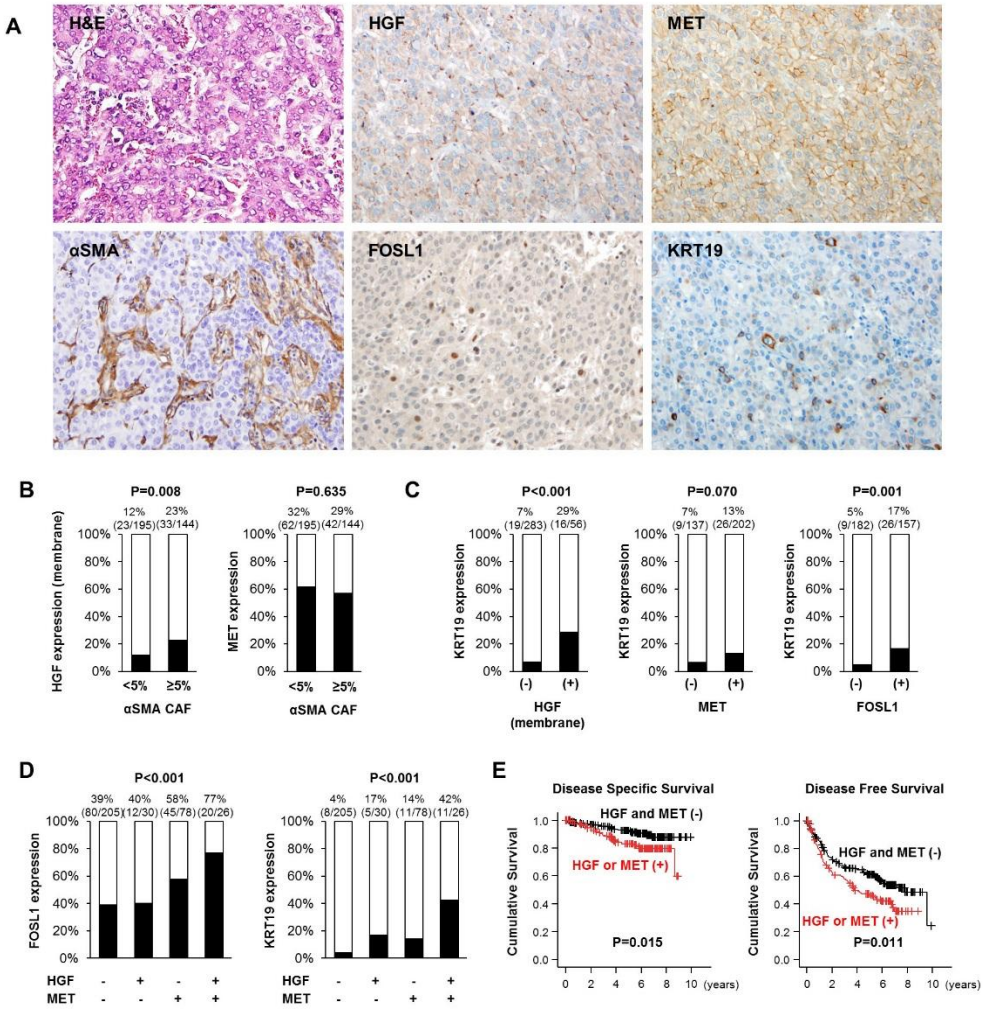

Figure 17. FOSL1 and KRT19 expression, and prognosis according to HGF/MET expression status. A) Representative hepatocellular carcinoma (HCC) tissue samples with positive expression of HGF, MET, FOSL1, and KRT19. B) The association between the αSMA-positive cancer-associated fibroblasts (≥5%) and HGF and MET expression. C) Association between KRT19 expression and HGF, MET, and FOSL1 expression. D) Expression of KRT19 in HCC patients subgrouped by HGF and MET status. E) Differences in disease-specific survival and disease-free survival between HGF or MET positive patients and HGF and MET-double negative patients.

IV. DISCUSSION

KRT19 is known as one of most important prognostic factors in HCC. However, the regulatory mechanism of KRT19 expression is not well understood, nor is why KRT19-positive HCC harbors aggressive behavior. To unveil the regulatory mechanisms of KRT19 expression, we began our study by focusing on the association between abundant fibrous stroma and KRT19 expression in HCC, establishing an *in vitro* model of fibroblasts and epithelial tumor cells using hepatic stellate cell and HCC cell lines, and exploring the mechanisms of the KRT19 expression. Our study demonstrated that KRT19 in HCC is regulated by cancer-associated fibroblast-derived HGF through a MET-ERK1/2-AP1 and SP1 axis. (Figure 18). Our results highlight the molecular background of clinically aggressive KRT19-positive HCC.

Previously, several studies have demonstrated the regulatory mechanisms of KRT19 expression in breast and pancreatic cancer cell lines.[38,39] In a pancreas cancer cell line model, SP1 and KLF4 were reported to be important transcriptional regulators of KRT19, and in a breast cancer cell line model, HER2 was reported to be an important upstream regulator of KRT19. Nevertheless, these studies had several limitations: for one, they used relatively short (less than 2 kbp) mouse KRT19 promoter constructs to search for transcriptional activators.[40] Notwithstanding, because the expression of HER2 expression in HCC is not as high as breast cancer, these mechanisms may not to be a sufficient answer for KRT19 regulatory mechanisms in HCC.[41]

In our study, AP1 (JUN/FOSL1 complex) and SP1 transcription factors were identified as crucial positive regulators of KRT19 in HCC. SP1 was also reported as a transcriptional activator of mouse KRT19 promoter,[38] and a previously reported SP1 binding site in mouse KRT19 promoter was homologous with the SP1 binding site that we found in human KRT19 promoter (Figure 19). To our knowledge, the AP1 binding site at 2kb upstream from the transcription start site has not been described previously. Interestingly, the AP1 binding site is very well conserved in most mammals, and the AP1 binding conservation is as well as protein coding region of

KRT19 (Figure 19), suggesting the functional importance of AP1-driven regulation of KRT19.

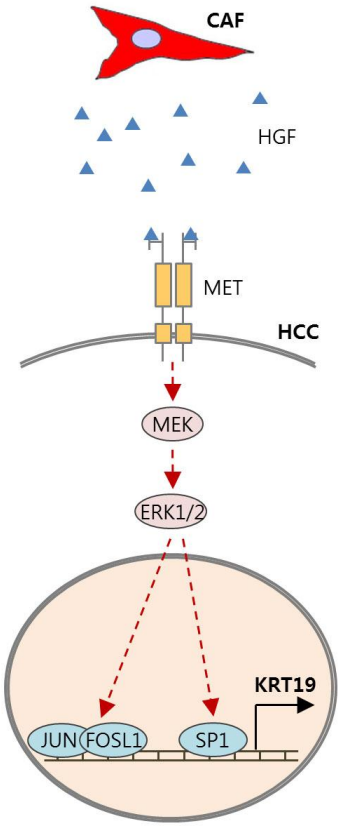

Figure 18. Schematic representation of regulatory mechanism of KRT19 gene by cancer-associated fibroblast (CAF) derived HGF via MET-ERK1/2-AP1/SP1 axis.

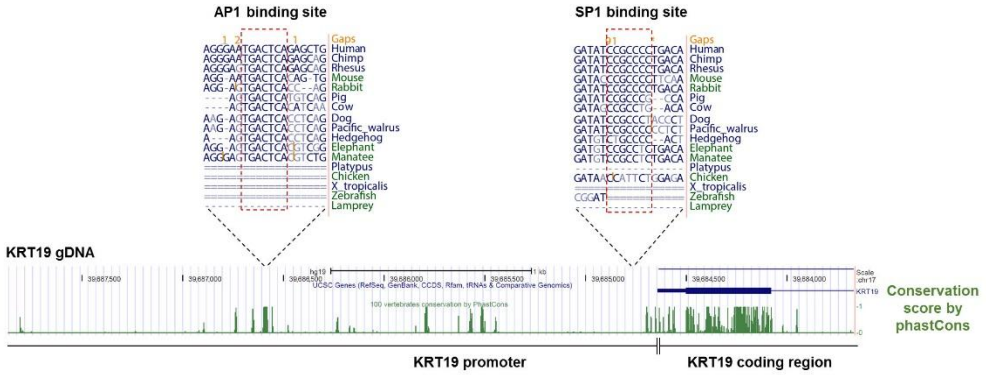

Figure 19. Conservation of AP1 and SP1 binding sites in KRT19 promoter. The conservation status of the promoter and first exon and intron of KRT19. The figure was modified from the UCSC genome browser (http://genome.ucsc.edu). The conservation score was calculated from 100 vertebrate species, measured by phastCons from the PHAST package. Multiple alignment of representative mammals and other vertebrae also exhibited the conservation status of AP1 and SP1 sites.

Previously, it was reported that a subset of HCC that exhibits a progenitor-like gene expression pattern, namely hepatoblast signature, comprises a poor prognosis.[42] In the aforementioned study, HCC with hepatoblast signature was highly expressed in hepatic stem cells, as was KRT19, and AP1 transcription factor was suggested as a major driver of hepatoblast signature expression. Our results provide a functional connection between HCC with hepatoblast signature, AP1 transcription factor, and KRT19 expression. Recently, a study demonstrated the tumor-initiating capacity of HCC is regulated by cancer-associated fibroblast-derived HGF and a MET-FOSL1 axis.[43] Collectively, previous and current reports seem to suggest the importance of MET/HGF and AP1 signaling axis in regulation of stemness of HCC, as well as the value of KRT19 as a marker of stemness and tumor-initiating capacity.

MET is an emerging therapeutic target of HCC, and currently, several clinical trials are targeting the HGF/MET signaling axis.[44] For optimal therapeutic application of MET inhibitors, selective enroll of patients with MET-addicted HCC is crucial. Unfortunately, there has been no validated immunohistochemical protocol with which to assess the activation status of MET.[45] Considering the short half-life (less than 10 mins) of phospho-MET, which we noted in our *in vitro* models, we doubt that a reliable assessment of the phosphorylation status of MET could be performed in clinical samples, especially in paraffin-embedded ones. Instead, we suggest that membranous distribution of MET and HGF and relatively stable downstream targets, including FOSL1 and KRT19, could serve as indirect markers of MET signaling activation.

In both our *in vitro* model and human HCC samples, HGF was mainly observed in epithelial tumor cells, not in cancer-associated fibroblasts, from which HGF is produced. However, subcellular distributions of HGF and MET differed between the *in vitro* and tissue samples: HGF and MET were mainly observed in intracellular space with the HCC cell lines and in the membrane of human HCC samples. The difference in subcellular location of HGF and MET might result from different dynamics in endocytosis-recycling of MET. The endocytosis of receptor tyrosine kinases is an important regulator of downstream signaling, and the endocytic pathway

is commonly deregulated in cancers.[46] The dynamics of endocytosis and recycling of MET has been shown to play a significant role in signal output of MET and MET-driven tumorigenesis.[47,48] Further study is needed to outline MET trafficking in HCC and its role in MET signaling.

V. CONCLUSION

The expression of KRT19 in HCC is regulated by cancer-associated fibroblasts in HCC via a HGF-MET-ERK1/2-AP1 and SP1 axis. The positive immunohistochemical staining of HGF and/or MET in human HCC was correlated with expression of FOSL1 and KRT19. Our results provide insights into the molecular background of aggressive KRT19-positive HCC. The assessment of these markers could serve as activation markers for MET signaling and poor outcomes.

REFERENCES

1. Bragulla HH, Homberger DG. Structure and functions of keratin proteins in simple, stratified, keratinized and cornified epithelia. Journal of Anatomy 2009;214:516-59.
2. Ku NO, Zhou X, Toivola DM, Omary MB. The cytoskeleton of digestive epithelia in health and disease. Am J Physiol 1999;277:G1108-37.
3. Moll R, Franke WW, Schiller DL, Geiger B, Krepler R. The catalog of human cytokeratins: patterns of expression in normal epithelia, tumors and cultured cells. Cell 1982;31:11-24.
4. Omary MB, Ku NO, Strnad P, Hanada S. Toward unraveling the complexity of simple epithelial keratins in human disease. J Clin Invest 2009;119:1794-805.
5. Roskams T, De Vos R, Van Eyken P, Myazaki H, Van Damme B, Desmet V. Hepatic OV-6 expression in human liver disease and rat experiments: evidence for hepatic progenitor cells in man. J Hepatol 1998;29:455-63.
6. Durnez A, Verslype C, Nevens F, Fevery J, Aerts R, Pirenne J, et al. The clinicopathological and prognostic relevance of cytokeratin 7 and 19 expression in hepatocellular carcinoma. A possible progenitor cell origin. Histopathology 2006;49:138-51.
7. Uenishi T, Kubo S, Yamamoto T, Shuto T, Ogawa M, Tanaka H, et al. Cytokeratin 19 expression in hepatocellular carcinoma predicts early postoperative recurrence. Cancer Sci 2003;94:851-7.
8. Kim H, Choi GH, Na DC, Ahn EY, Kim GI, Lee JE, et al. Human hepatocellular carcinomas with "Stemness"-related marker expression: keratin 19 expression and a poor prognosis. Hepatology 2011;54:1707-17.
9. Govaere O, Komuta M, Berkers J, Spee B, Janssen C, de Luca F, et al. Keratin 19: a key role player in the invasion of human hepatocellular carcinomas. Gut 2014;63:674-85.
10. Yang XR, Xu Y, Yu B, Zhou J, Qiu SJ, Shi GM, et al. High expression levels

of putative hepatic stem/progenitor cell biomarkers related to tumour angiogenesis and poor prognosis of hepatocellular carcinoma. Gut 2010;59:953-62.

11. Tsuchiya K, Komuta M, Yasui Y, Tamaki N, Hosokawa T, Ueda K, et al. Expression of keratin 19 is related to high recurrence of hepatocellular carcinoma after radiofrequency ablation. Oncology 2011;80:278-88.
12. Rhee H, Nahm JH, Kim H, Choi GH, Yoo JE, Lee HS, et al. Poor outcome of hepatocellular carcinoma with stemness marker under hypoxia: resistance to transarterial chemoembolization. Mod Pathol 2016;29:1038-49.
13. Miltiadous O, Sia D, Hoshida Y, Fiel MI, Harrington AN, Thung SN, et al. Progenitor cell markers predict outcome of patients with hepatocellular carcinoma beyond Milan criteria undergoing liver transplantation. J Hepatol 2015;63:1368-77.
14. Bruix J, Sherman M. Management of hepatocellular carcinoma: an update. Hepatology 2011;53:1020-2.
15. European Association For The Study Of The L, European Organisation For R, Treatment Of C. EASL-EORTC clinical practice guidelines: management of hepatocellular carcinoma. J Hepatol 2012;56:908-43.
16. Roskams T. Liver stem cells and their implication in hepatocellular and cholangiocarcinoma. Oncogene 2006;25:3818-22.
17. Kowalik MA, Sulas P, Ledda-Columbano GM, Giordano S, Columbano A, Perra A. Cytokeratin-19 positivity is acquired along cancer progression and does not predict cell origin in rat hepatocarcinogenesis. Oncotarget 2015;6:38749-63.
18. Mu X, Espanol-Suner R, Mederacke I, Affo S, Manco R, Sempoux C, et al. Hepatocellular carcinoma originates from hepatocytes and not from the progenitor/biliary compartment. J Clin Invest 2015;125:3891-903.
19. Seok JY, Na DC, Woo HG, Roncalli M, Kwon SM, Yoo JE, et al. A fibrous stromal component in hepatocellular carcinoma reveals a cholangiocarcinoma-like gene expression trait and epithelial-mesenchymal

transition. Hepatology 2012;55:1776-86.

20. Gascard P, Tlsty TD. Carcinoma-associated fibroblasts: orchestrating the composition of malignancy. Genes & Development 2016;30:1002-19.
21. Mazzocca A, Dituri F, Lupo L, Quaranta M, Antonaci S, Giannelli G. Tumor-secreted lysophostatidic acid accelerates hepatocellular carcinoma progression by promoting differentiation of peritumoral fibroblasts in myofibroblasts. Hepatology 2011;54:920-30.
22. Novo E, di Bonzo LV, Cannito S, Colombatto S, Parola M. Hepatic myofibroblasts: a heterogeneous population of multifunctional cells in liver fibrogenesis. Int J Biochem Cell Biol 2009;41:2089-93.
23. Friedman SL. Hepatic stellate cells: protean, multifunctional, and enigmatic cells of the liver. Physiol Rev 2008;88:125-72.
24. Schnabl B, Choi YH, Olsen JC, Hagedorn CH, Brenner DA. Immortal activated human hepatic stellate cells generated by ectopic telomerase expression. Lab Invest 2002;82:323-33.
25. Xu L, Hui AY, Albanis E, Arthur MJ, O'Byrne SM, Blaner WS, et al. Human hepatic stellate cell lines, LX-1 and LX-2: new tools for analysis of hepatic fibrosis. Gut 2005;54:142-51.
26. Guan B, Wang TL, Shih Ie M. ARID1A, a factor that promotes formation of SWI/SNF-mediated chromatin remodeling, is a tumor suppressor in gynecologic cancers. Cancer Res 2011;71:6718-27.
27. Wiederschain D, Wee S, Chen L, Loo A, Yang G, Huang A, et al. Single-vector inducible lentiviral RNAi system for oncology target validation. Cell Cycle 2009;8:498-504.
28. Bakiri L, Matsuo K, Wisniewska M, Wagner EF, Yaniv M. Promoter specificity and biological activity of tethered AP-1 dimers. Mol Cell Biol 2002;22:4952-64.
29. Nault JC, De Reynies A, Villanueva A, Calderaro J, Rebouissou S, Couchy G, et al. A hepatocellular carcinoma 5-gene score associated with survival of patients after liver resection. Gastroenterology 2013;145:176-87.

30. Jia CC, Wang TT, Liu W, Fu BS, Hua X, Wang GY, et al. Cancer-associated fibroblasts from hepatocellular carcinoma promote malignant cell proliferation by HGF secretion. PLoS One 2013;8:e63243.
31. Morris EJ, Jha S, Restaino CR, Dayananth P, Zhu H, Cooper A, et al. Discovery of a novel ERK inhibitor with activity in models of acquired resistance to BRAF and MEK inhibitors. Cancer Discov 2013;3:742-50.
32. Brunet A, Pages G, Pouyssegur J. Constitutively active mutants of MAP kinase kinase (MEK1) induce growth factor-relaxation and oncogenicity when expressed in fibroblasts. Oncogene 1994;9:3379-87.
33. Neaud V, Faouzi S, Guirouilh J, Le Bail B, Balabaud C, Bioulac- Sage P, et al. Human hepatic myofibroblasts increase invasiveness of hepatocellular carcinoma cells: evidence for a role of hepatocyte growth factor. Hepatology 1997;26:1458-66.
34. Eferl R, Wagner EF. AP-1: a double-edged sword in tumorigenesis. Nat Rev Cancer 2003;3:859-68.
35. Basbous J, Chalbos D, Hipskind R, Jariel-Encontre I, Piechaczyk M. Ubiquitin-independent proteasomal degradation of Fra-1 is antagonized by Erk1/2 pathway-mediated phosphorylation of a unique C-terminal destabilizer. Mol Cell Biol 2007;27:3936-50.
36. Zou HY, Li Q, Lee JH, Arango ME, McDonnell SR, Yamazaki S, et al. An orally available small-molecule inhibitor of c-Met, PF-2341066, exhibits cytoreductive antitumor efficacy through antiproliferative and antiangiogenic mechanisms. Cancer research 2007;67:4408-17.
37. Wilhelm SM, Carter C, Tang L, Wilkie D, McNabola A, Rong H, et al. BAY 43-9006 exhibits broad spectrum oral antitumor activity and targets the RAF/MEK/ERK pathway and receptor tyrosine kinases involved in tumor progression and angiogenesis. Cancer research 2004;64:7099-109.
38. Brembeck FH, Rustgi AK. The tissue-dependent keratin 19 gene transcription is regulated by GKLF/KLF4 and Sp1. J Biol Chem 2000;275:28230-9.

39. Ju JH, Oh S, Lee KM, Yang W, Nam KS, Moon HG, et al. Cytokeratin19 induced by HER2/ERK binds and stabilizes HER2 on cell membranes. Cell Death Differ 2014.
40. Lussier M, Filion M, Compton JG, Nadeau JH, Lapointe L, Royal A. The mouse keratin 19-encoding gene: sequence, structure and chromosomal assignment. Gene 1990;95:203-13.
41. Xian ZH, Zhang SH, Cong WM, Wu WQ, Wu MC. Overexpression/amplification of HER-2/neu is uncommon in hepatocellular carcinoma. J Clin Pathol 2005;58:500-3.
42. Lee JS, Heo J, Libbrecht L, Chu IS, Kaposi-Novak P, Calvisi DF, et al. A novel prognostic subtype of human hepatocellular carcinoma derived from hepatic progenitor cells. Nat Med 2006;12:410-6.
43. Lau EY, Lo J, Cheng BY, Ma MK, Lee JM, Ng JK, et al. Cancer-Associated Fibroblasts Regulate Tumor-Initiating Cell Plasticity in Hepatocellular Carcinoma through c-Met/FRA1/HEY1 Signaling. Cell Rep 2016;15:1175-89.
44. Qi XS, Guo XZ, Han GH, Li HY, Chen J. MET inhibitors for treatment of advanced hepatocellular carcinoma: A review. World J Gastroenterol 2015;21:5445-53.
45. Giordano S, Columbano A. Met as a therapeutic target in HCC: facts and hopes. J Hepatol 2014;60:442-52.
46. Mellman I, Yarden Y. Endocytosis and Cancer. Cold Spring Harbor Perspectives in Biology 2013;5.
47. Kermorgant S, Parker PJ. Receptor trafficking controls weak signal delivery: a strategy used by c-Met for STAT3 nuclear accumulation. The Journal of Cell Biology 2008;182:855-63.
48. Joffre C, Barrow R, Ménard L, Calleja V, Hart IR, Kermorgant S. A direct role for Met endocytosis in tumorigenesis. Nature Cell Biology 2011;13:827-37.

ABSTRACT (IN KOREAN)

간세포암에서 섬유아세포 유래 간세포성장인자와 MET-ERK1/2-AP1/SP1 신호전달에 의한 KRT19의 발현 조절

<지도교수 박영년>

연세대학교 대학원 의과학과

이형진

Keratin 19 (KRT19)는 간의 줄기세포/전구세포 표지자이며, 간암의 불량한 예후를 나타내는 인자로 잘 알려져 있음. 본 연구진은 풍부한 섬유성 기질을 가진 간암의 아형 (경화성 간암)에서 KRT19의 발현이 높음을 보고한 바 있음. 그러나, 간암에서 KRT19의 발현 조절 기전은 잘 알려져 있지 아니함.

본 연구에서는 간성상세포주(hTERT-HSC)와 간암세포주(HepG2, SNU423) 사이의 분비 인자 상호 작용 모델을 이용하여 KRT19의 발현 조절 기전을 연구하였음. 또한 KRT19의 조절 기전을 인체 간암 조직 339례로 구성된 조직미세배열에서 검증하였음.

간성상세포주(hTERT-HSC)은 분비 인자를 통하여 두 간암세포주에서 KRT19의 전사 및 단백질 발현을 증가시켰음. hTERT-HSC 유래 적응용배지에 포함된 간세포성장인자가 MET을 활성화시키며, 이에 따라 활성화된 MEK-ERK1/2 신호전달계에

의하여 KRT19의 발현이 증가함. 루시페레이즈를 이용한 촉진염기서열 분석을 통하여 KRT19 촉진염기서열 중 AP1과 SP1 전사인자 결합부위가 KRT19 조절에 중요함을 밝힘. ERK1/2 신호전달계의 하위에 있는 JUN과 FOSL1 등의 AP1 전사인자와 SP1 전사인자가 KRT19의 발현을 활성함을 밝힘. Sorafenib, crizotininb이 MET 또는 MEK-ERK1/2 신호전달계의 활성을 저해하여 적응용배지에 의한 KRT19 발현 증가를 저해할 수 있었음. 인체 간암 조직에서 면역 염색으로 단백질 발현을 확인한 결과, KRT19의 발현은 HGF, MET, FOSL1의 발현과 유의한 상관 관계를 보였으며, 간암에서 관찰된 암 연관 섬유아세포 양과도 유의한 상관을 보였음.

결론적으로, 간암에서 KRT19의 발현은 간암의 암 연관 섬유아세포에 의하여 HGF-MET-ERK1/2-AP1/SP1 신호전달을 통하여 조절됨. 본 연구 결과는 임상적으로 불량한 예후를 보이는 KRT19 양성 간암의 분자적 특성을 이해할 수 있도록 함.

핵심되는 말: Keratin 19, 암 연관 섬유아세포, 간세포성장인자, MET, Fos-related antigen 1

PUBLICATION LIST

1. Ahn E, Yoo J, **Rhee H**, Kim M, Choi J, Ko J, et al. Increased expression of stathmin and elongation factor 1α in precancerous nodules with telomere dysfunction in hepatitis B viral cirrhotic patients. Journal of Translational Medicine 2014;12:1-12.

2. Kim G, **Rhee H**, Yoo J, Ko J, Lee J, Kim H, et al. Increased Expression of CCN2, Epithelial Membrane Antigen, and Fibroblast Activation Protein in Hepatocellular Carcinoma with Fibrous Stroma Showing Aggressive Behavior. PLoS ONE 2014;9.

3. **Rhee H**, Nahm JH, Kim H, Choi GH, Yoo JE, Lee HS, et al. Poor outcome of hepatocellular carcinoma with stemness marker under hypoxia: resistance to transarterial chemoembolization. Mod Pathol 2016;29:1038-49.